



Huazhong University of Science & Technology



Design considerations of a superconducting gantry with alternating-gradient combined-function magnets

Bin Qin, Runxiao Zhao, Xu Liu

Institute of Applied Electromagnetic Engineering
Huazhong University of Science and Technology (HUST)

*International Conference on Medical Accelerators and Particle Therapy
Seville, Spain, September 4th, 2019*

OUTLINE

I. Introduction of HUST-PTF

II. Design of SC gantry with AG combined-function magnets

1. Overall considerations

2. Field imperfections of small-curvature AG-CCTs, and its influence

3. Design of a hybrid structure degrader

III. Conclusion

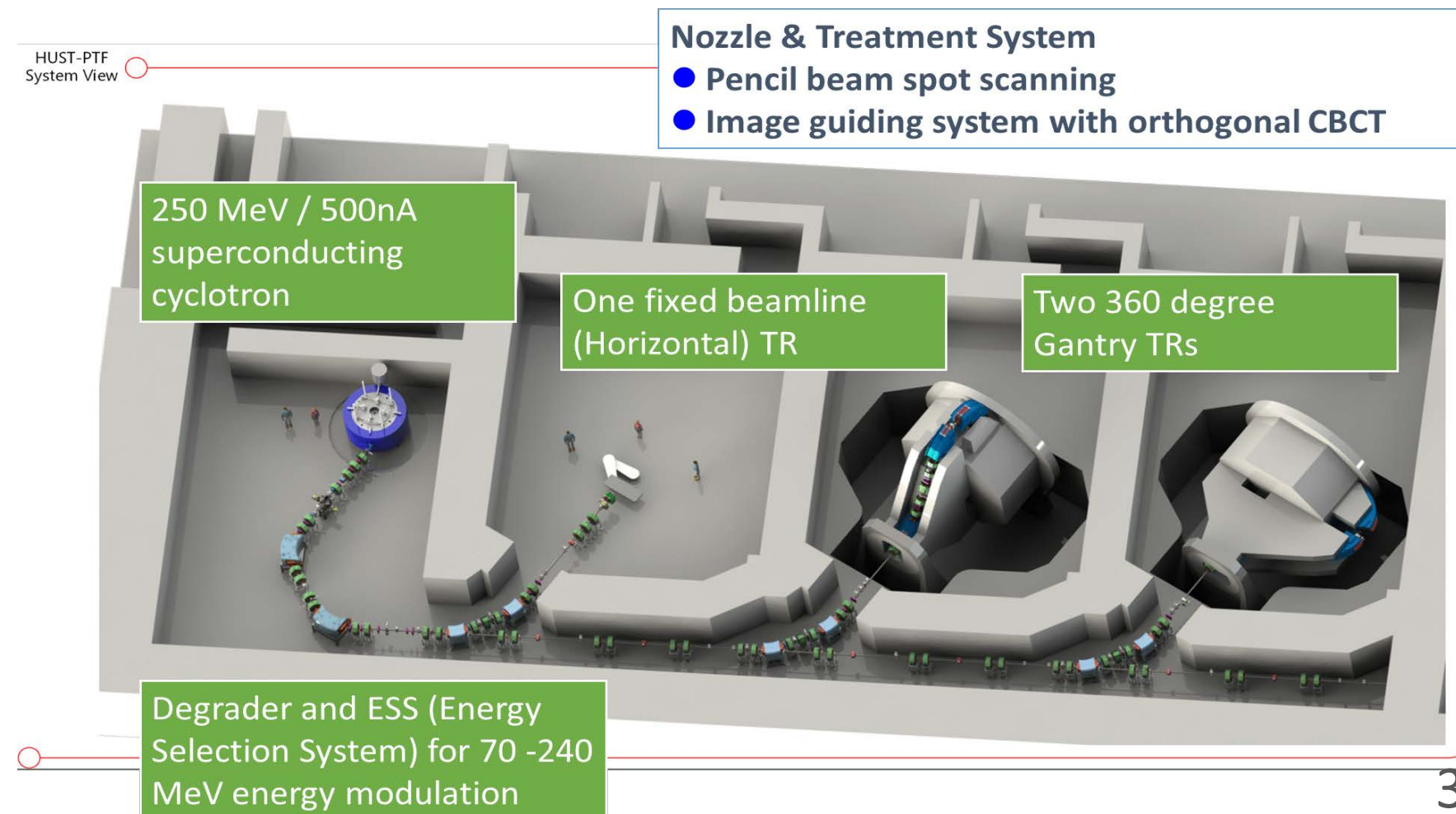
Introduction of HUST Proton Therapy Facility

■ At HUST (Huazhong University of Science and Technology, Wuhan, China), a multi-rooms proton therapy facility based on superconducting cyclotron, is under development.

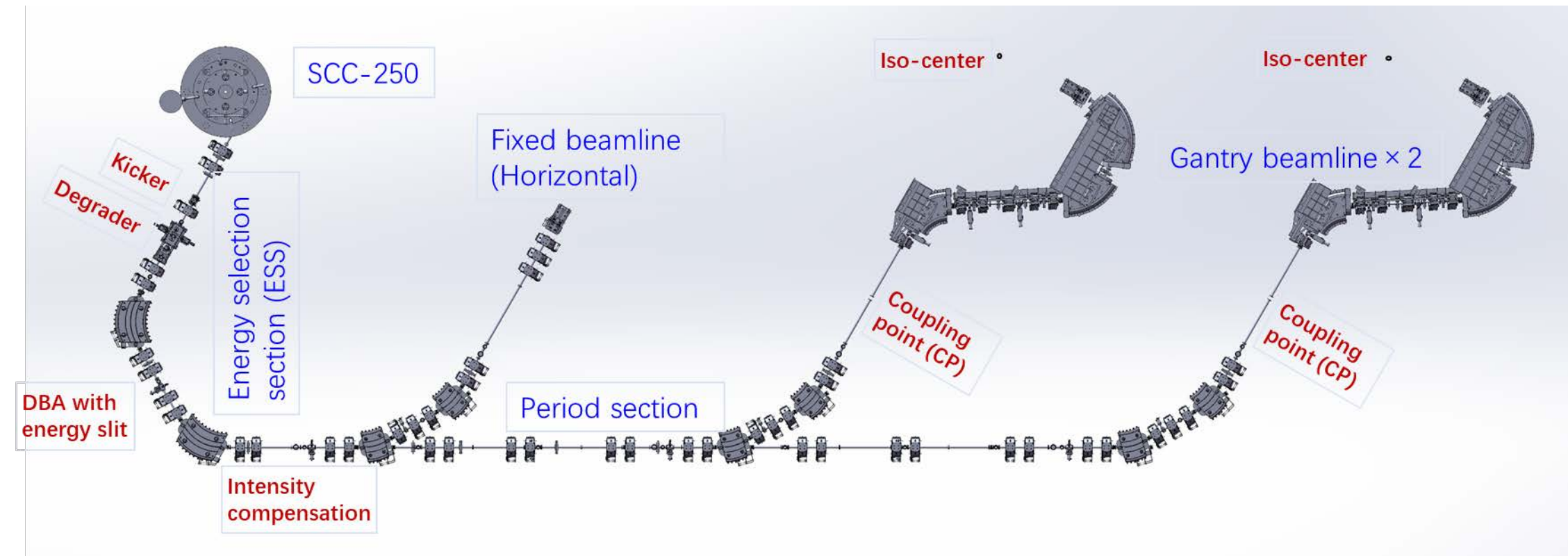


Main specifications

| Specification | Value |
|-----------------------------|---------------------------------------|
| Accelerator type | SC cyclotron (250 MeV) |
| Energy range of ESS | 70-240 MeV |
| Gantry type | ±180 degree, normal conducting |
| Scanning method | Downstream, pencil beam spot scanning |
| Virtual SAD | 2.6 m |
| Beam intensity @ Iso-center | 0.4 – 5 nA |
| Field size | 30cm × 30cm |
| Image guiding | Cone beam CT |

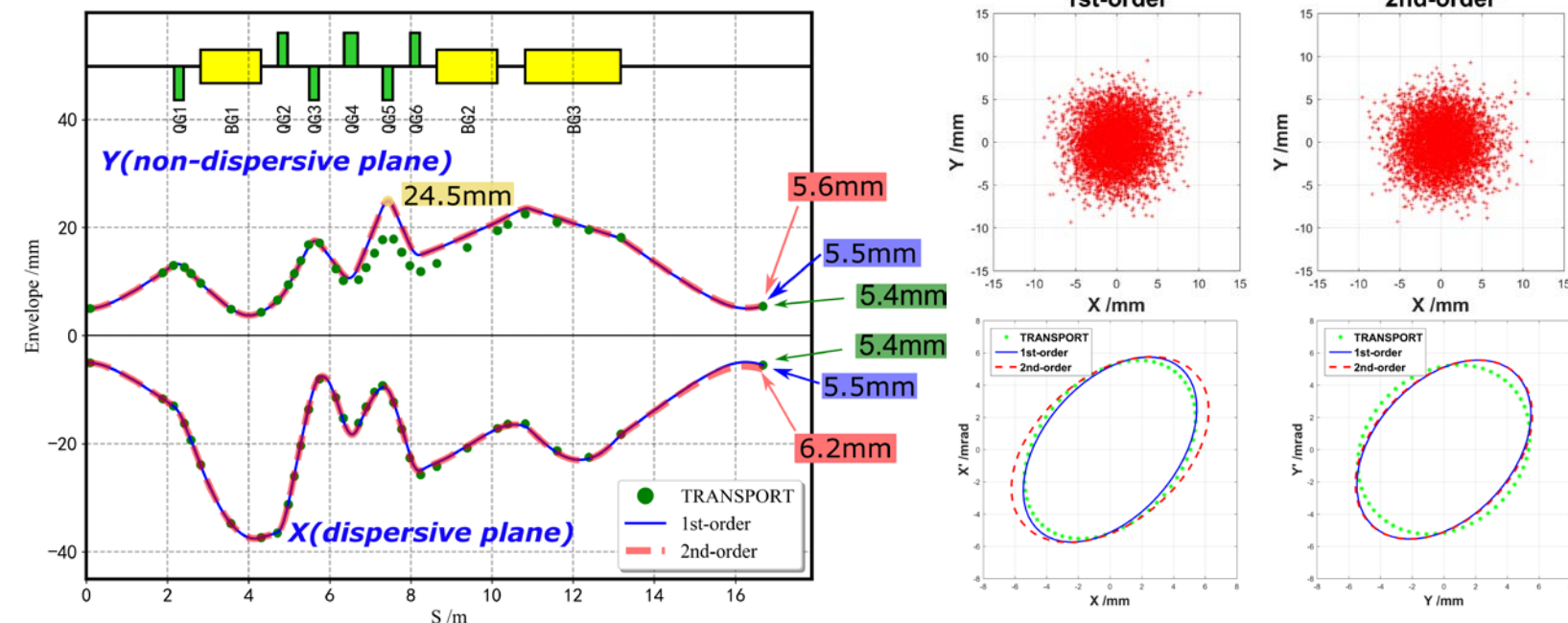
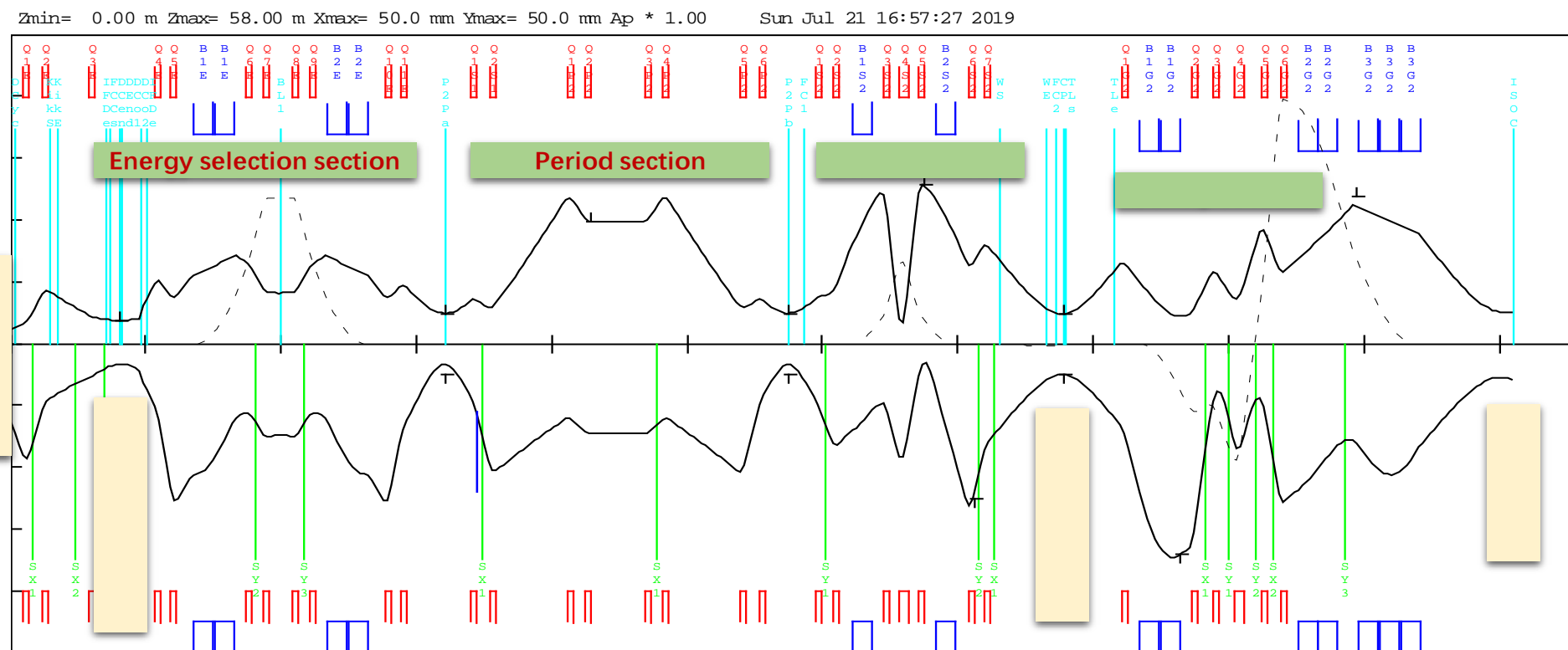


Beamline layout and resistive gantry



Gantry beamline with downstream scanning:

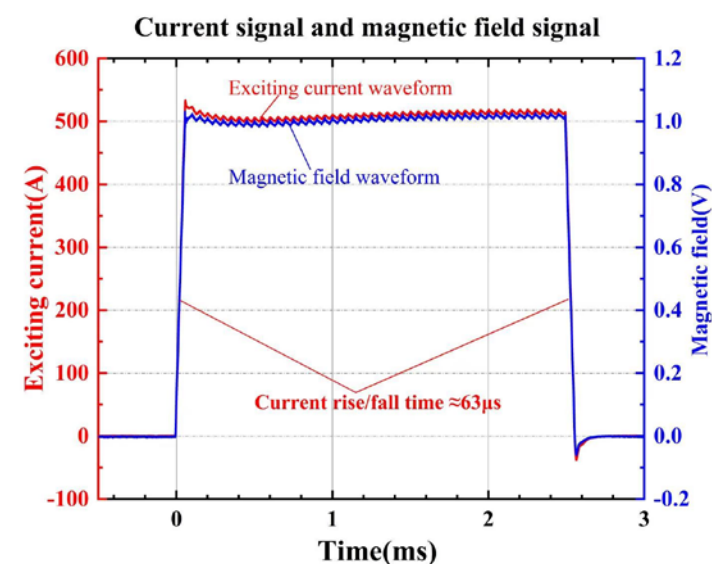
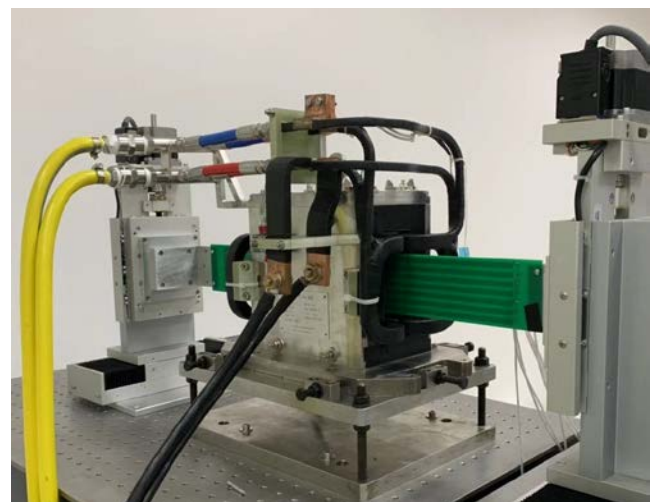
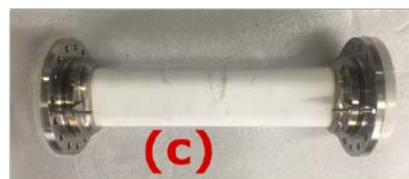
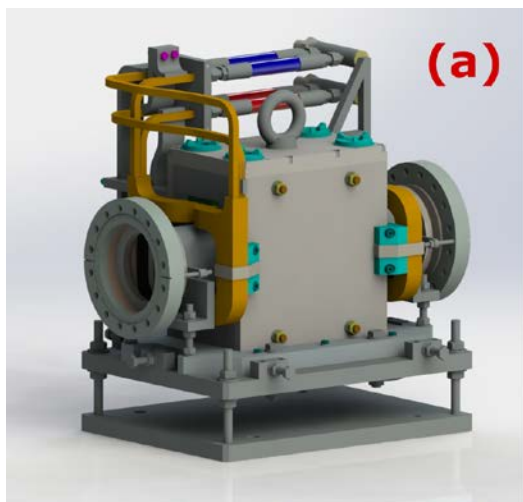
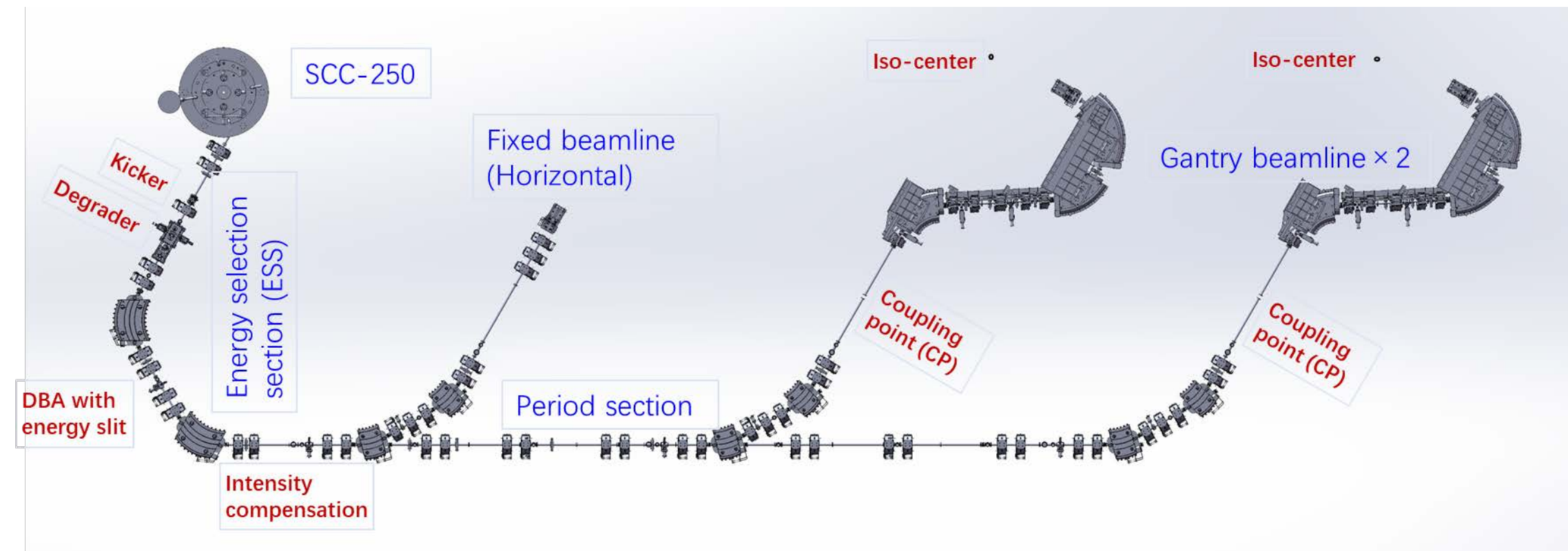
1. Image optics for better correlation between the iso-center and entrance CP;
2. Beam optics is optimized when considering fringe fields and 2nd order aberrations (COSY INFINITY with ENGE function / FEA-ODE code), and validated by tracking.



2 σ beam ($\epsilon_{x,y} = 28\pi \cdot \text{mm} \cdot \text{mrad}$, $\Delta p/p = \pm 0.6\%$) envelope calculated by Transport

Comparison of 2 σ beam envelope with Transport, first / second order results after optimization with COSY Infinity.

Beamline layout and resistive gantry



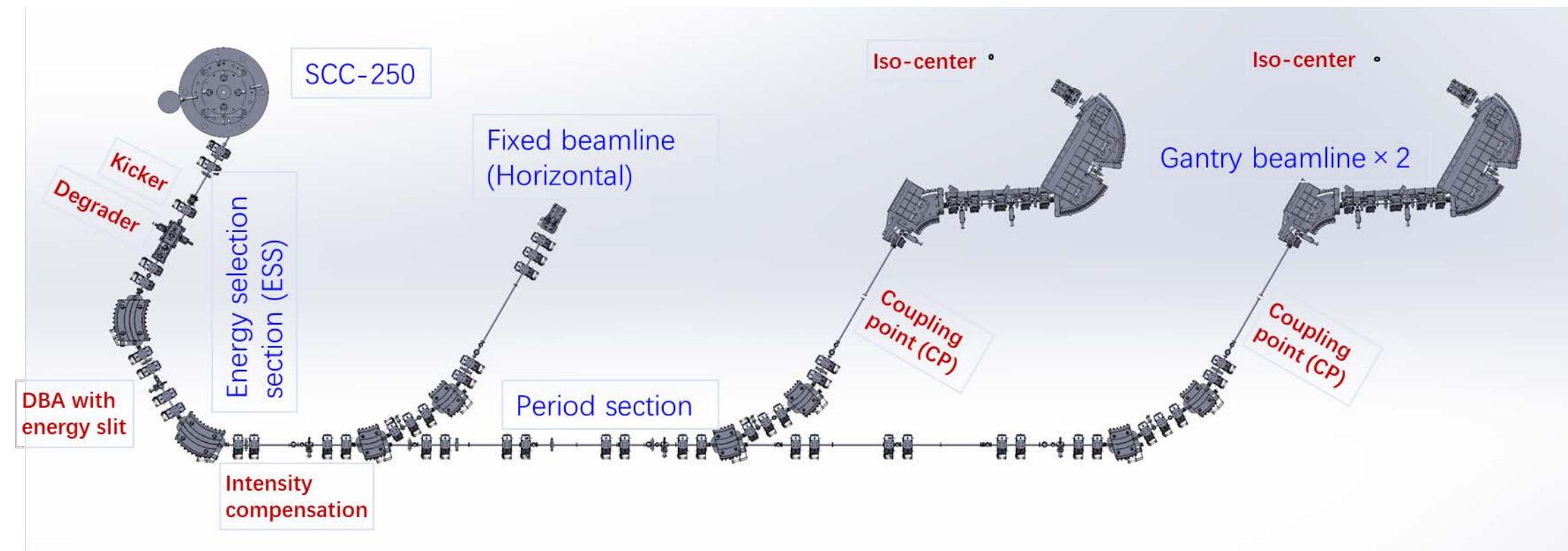
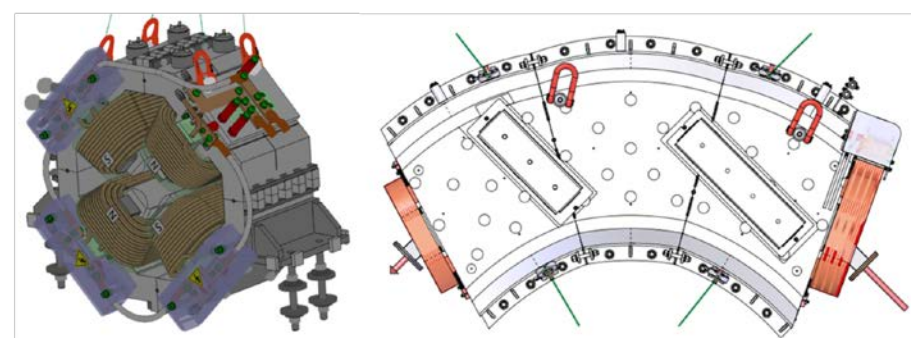
➤ Energy degrader: multi-wedge type for continuous and fast energy modulation (70 – 240 MeV, 200ms / step)

- Kicker magnet for fast beam switch : MnZn ferrite core + Ceramic vacuum chamber; rise / fall time 63 us (measured)
- Central field 1050Gs, field homogeneity 0.5% in GFR (measured)

Beamline layout and resistive gantry

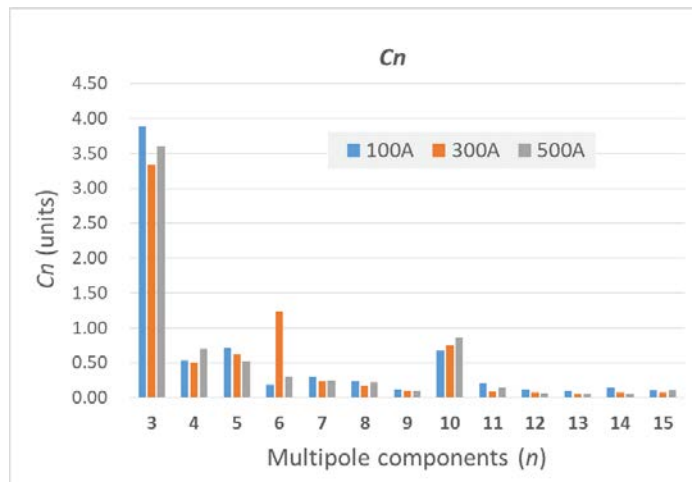
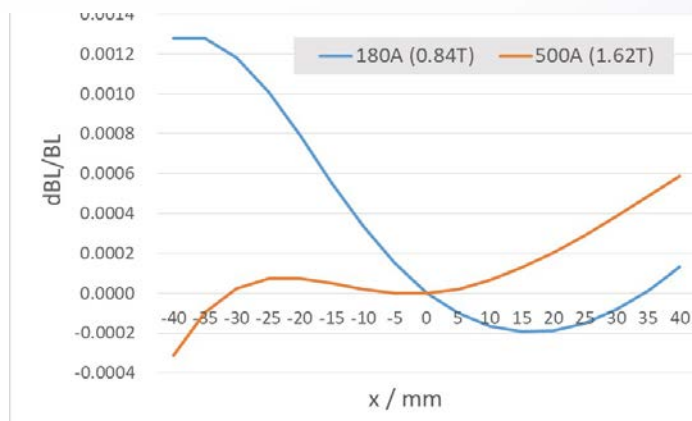
Gantry beamline

- Downstream scanning with field size 30cm × 30cm
- **Integrated design** for magnets, vacuum system, diagnostics and girders.
- **#1 gantry beamline will be manufactured and tested in the end of 2019.**



Prototype beamline magnets: 60° dipole; L270 mm quadrupole; 30° dipole

- Max. dipole field 1.62T, with integral field homogeneity $\pm 0.08\%$
- Max. quadrupole gradient 18T/m, high order harmonics < 5 units





OUTLINE

I. Introduction of HUST-PTF

II. Design of SC gantry with AG combined-function magnets

1. Overall considerations

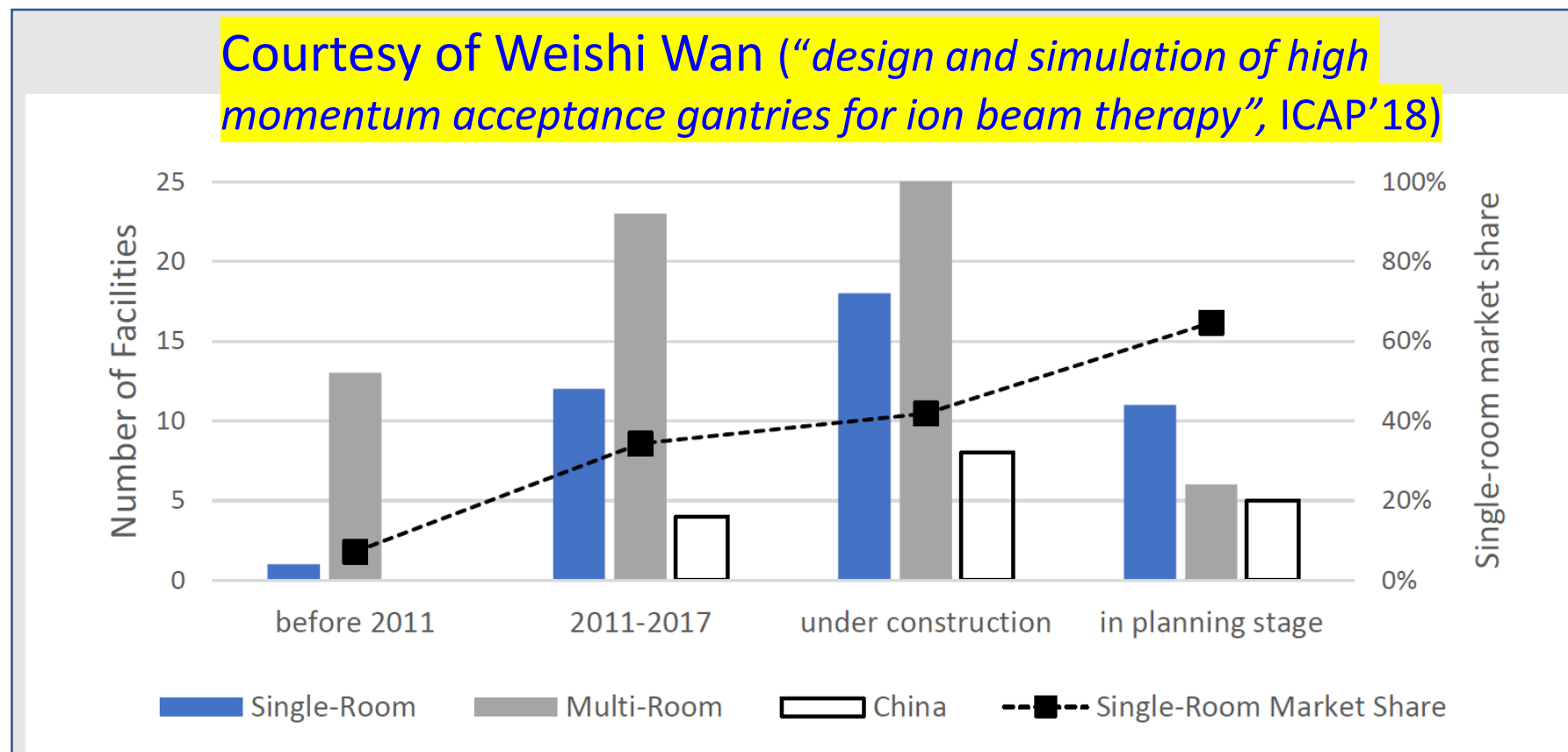
2. Field imperfections of small-curvature AG-CCTs, and its influence

3. Design of a hybrid structure degrader

III. Conclusions

Motivation

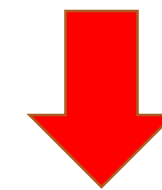
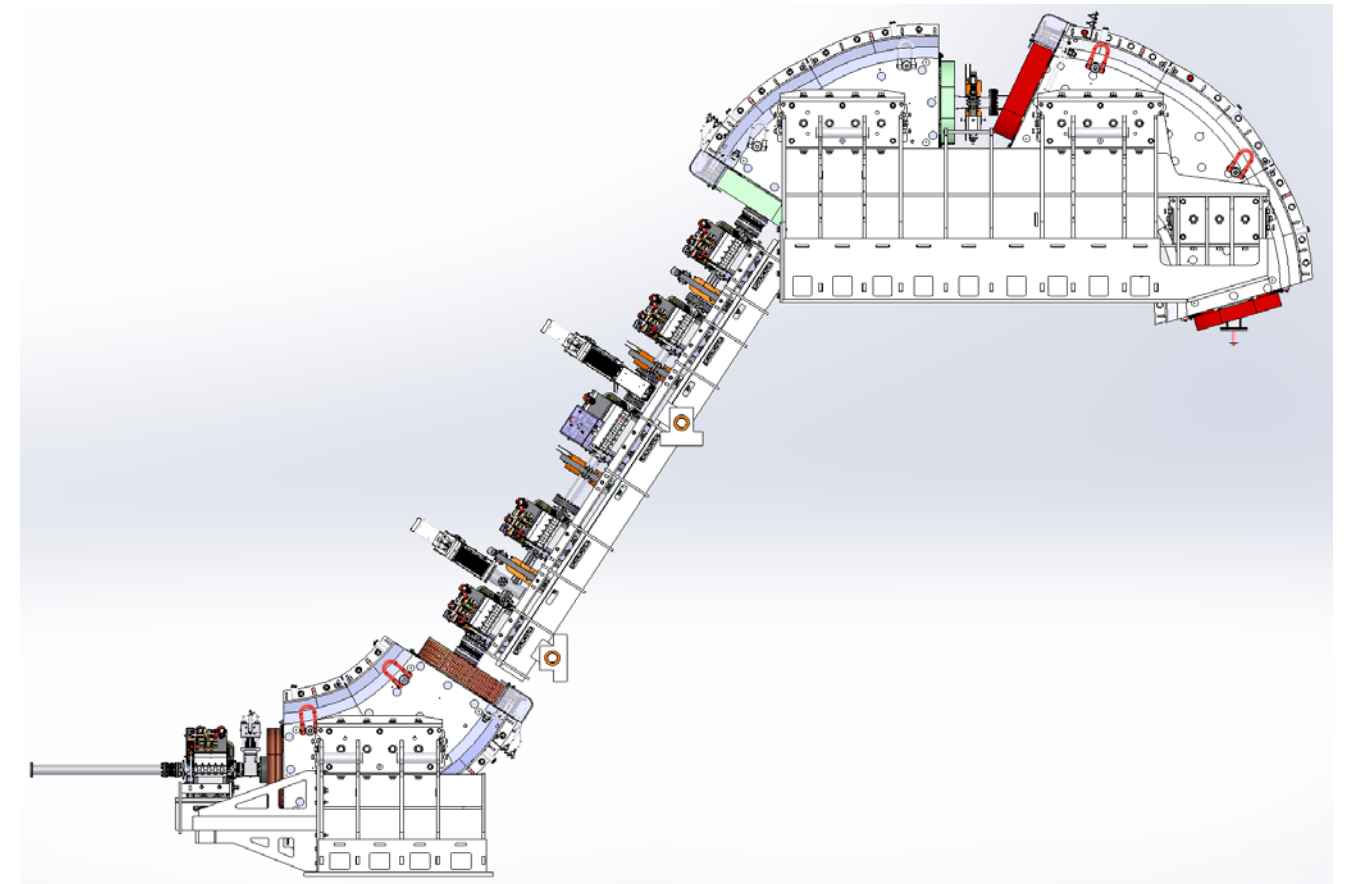
- Single room compact PT system becomes attractive for radiotherapy markets: **16 of 44 PT centers under constructions will adopt single-room solutions** (from <https://www.ptcog.ch>)



- SC cyclotrons / synchro-cyclotrons have been applied to PT, however, most of single-room and multi-room PTs employs resistive gantries. **SC technology can further suppress both the footprint and weight of gantries.**

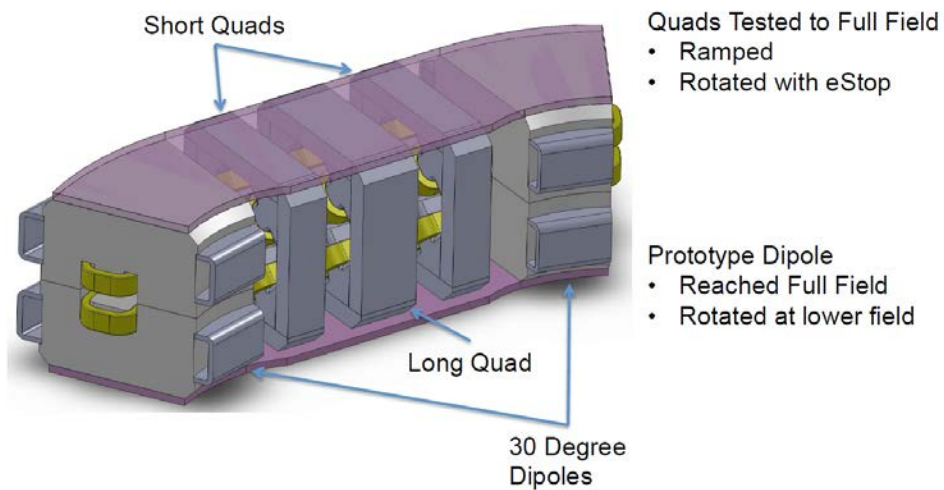
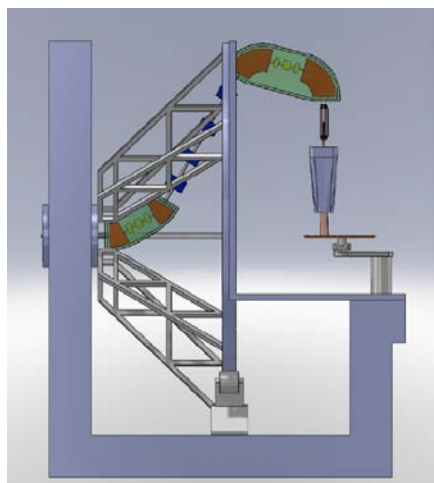
Present resistive gantry beamline of HUST-PTF

- Weight of beamline (magnets + girders) ~ 35 tons
- Overall gantry weight: ~ 180 tons
- Footprint: ~ 5m (R) × 8m (L)



A lightweight gantry is considered for future upgrade

Existing schemes of SC gantries (PT)



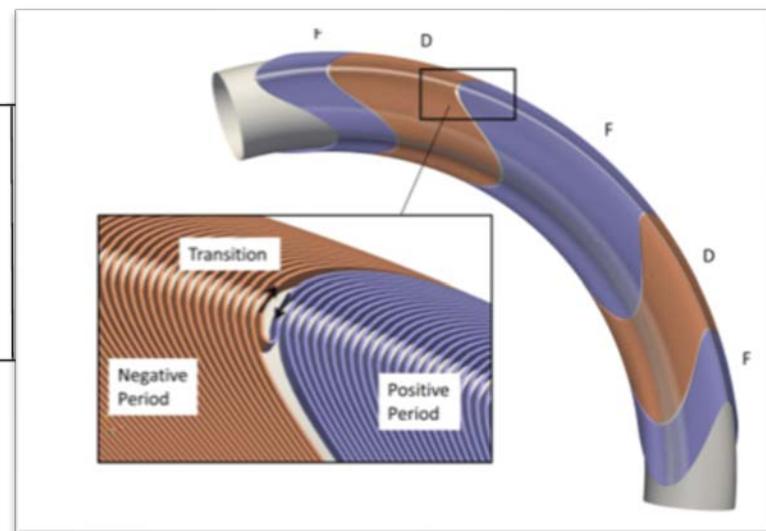
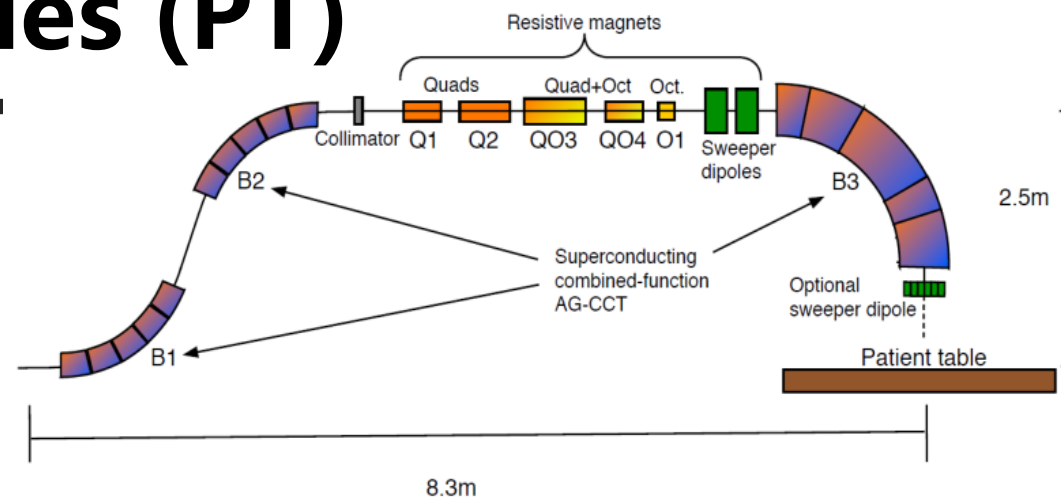
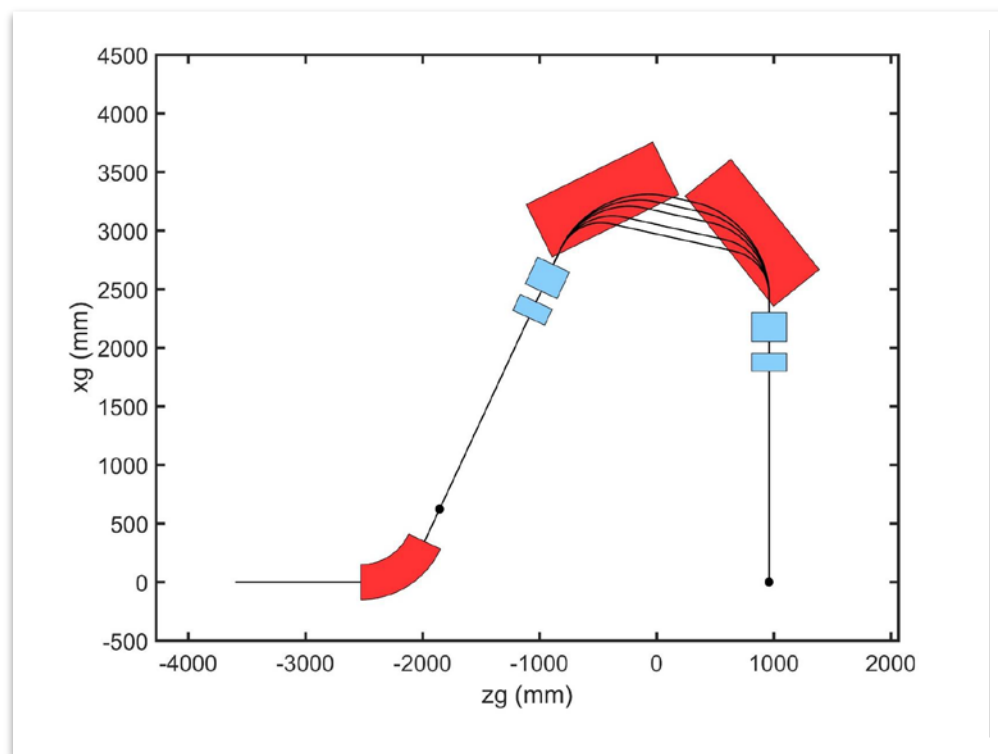
□ ProNova Super-ferric scheme

- Combined super-ferric magnets, +/-3% momentum acceptance
- Commercial available, 30 tons lightweight gantry

-- L. Derenchuk, The ProNova SC360 Gantry, Modern Hadron Therapy Gantry Workshop, 2014

□ Fixed field dipole scheme

-- Anthony Huggins, Lucas Brouwer, Weishi Wan, Design and simulation of high momentum acceptance gantries for ion beam therapy, ICAP'18, 2018

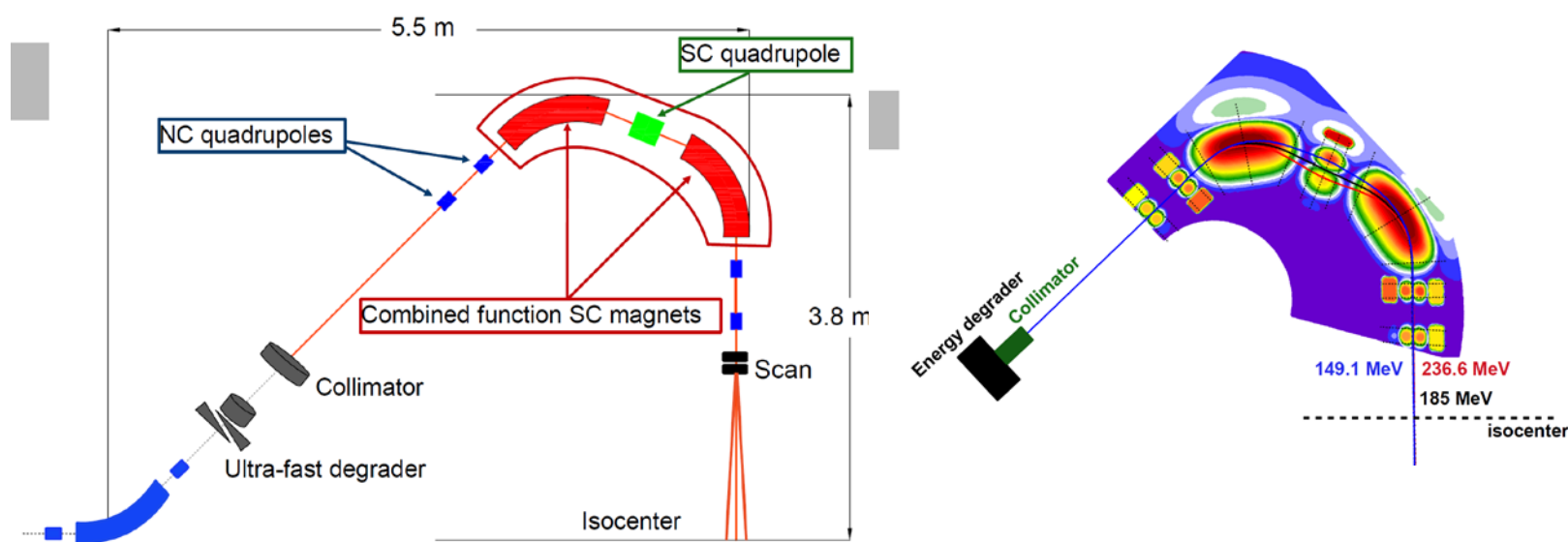


□ LBNL / PSI: AG-CCT Scheme

- Dipole CCT + AG-CCT, stronger dispersion suppression: +/- 10% momentum acceptance;
- Upstream scanning, larger aperture for the final dipole

-- W. Wan et al. Beam Optics in Large Aperture Magnets, EuCARD2, 2015

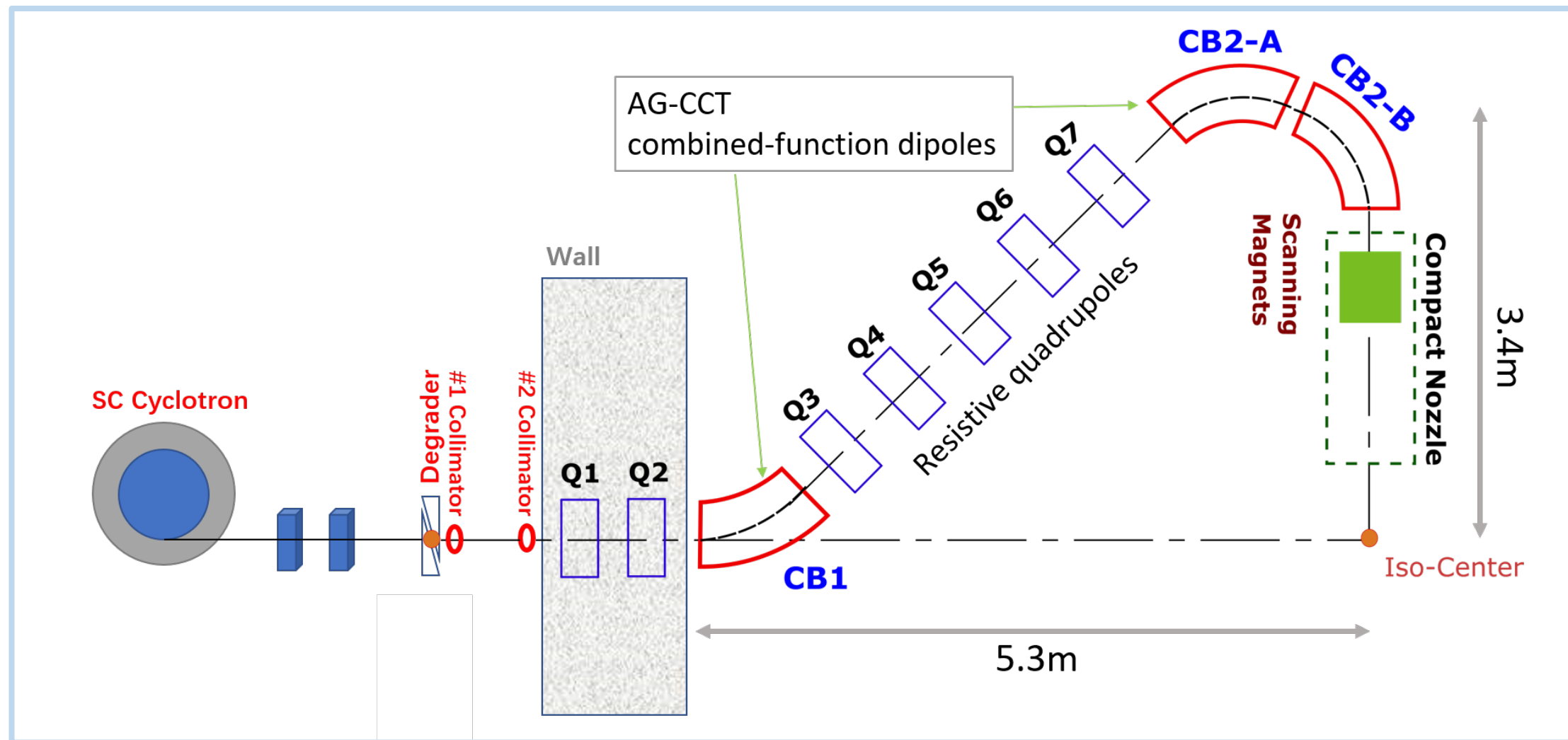
-- L. Brouwer et al.: Design of an achromatic superconducting magnet for a proton therapy gantry, IEEE TAS, VOL. 27, NO. 4, JUNE 2017



□ PSI combined-function SC magnet scheme: +/-15% momentum acceptance

-- Konrad P. Nesteruk. Large momentum acceptance beam optics of a superconducting gantry for proton therapy, CPO-10, 2018

Schematic design of the downstream scanning AG-CCT gantry



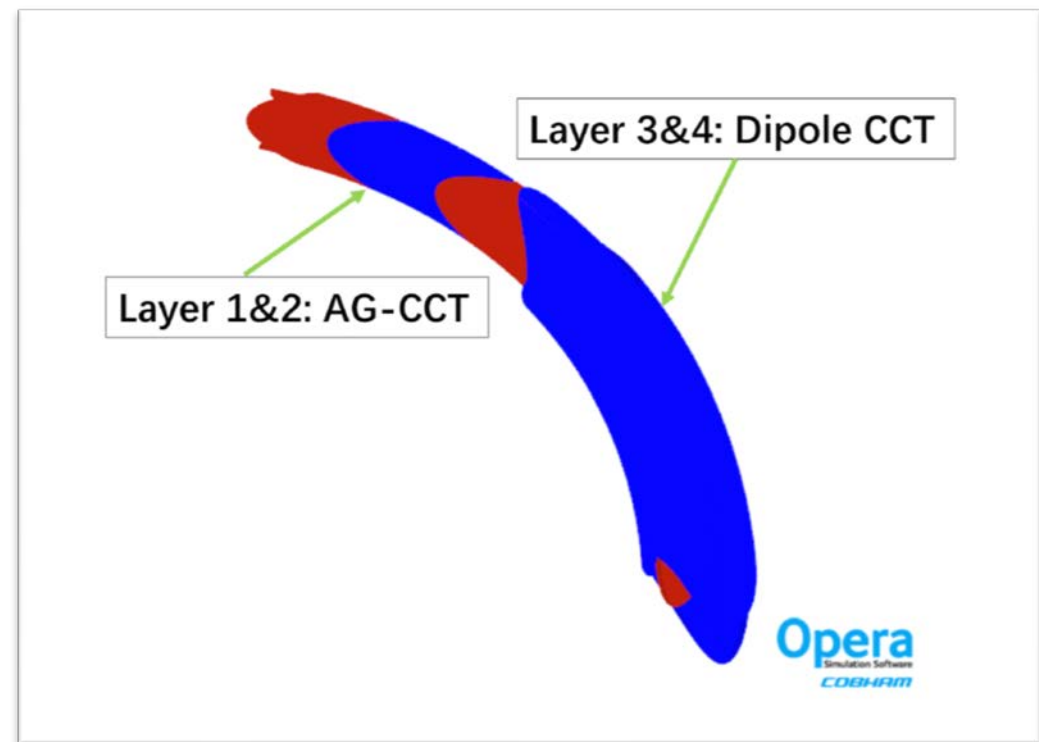
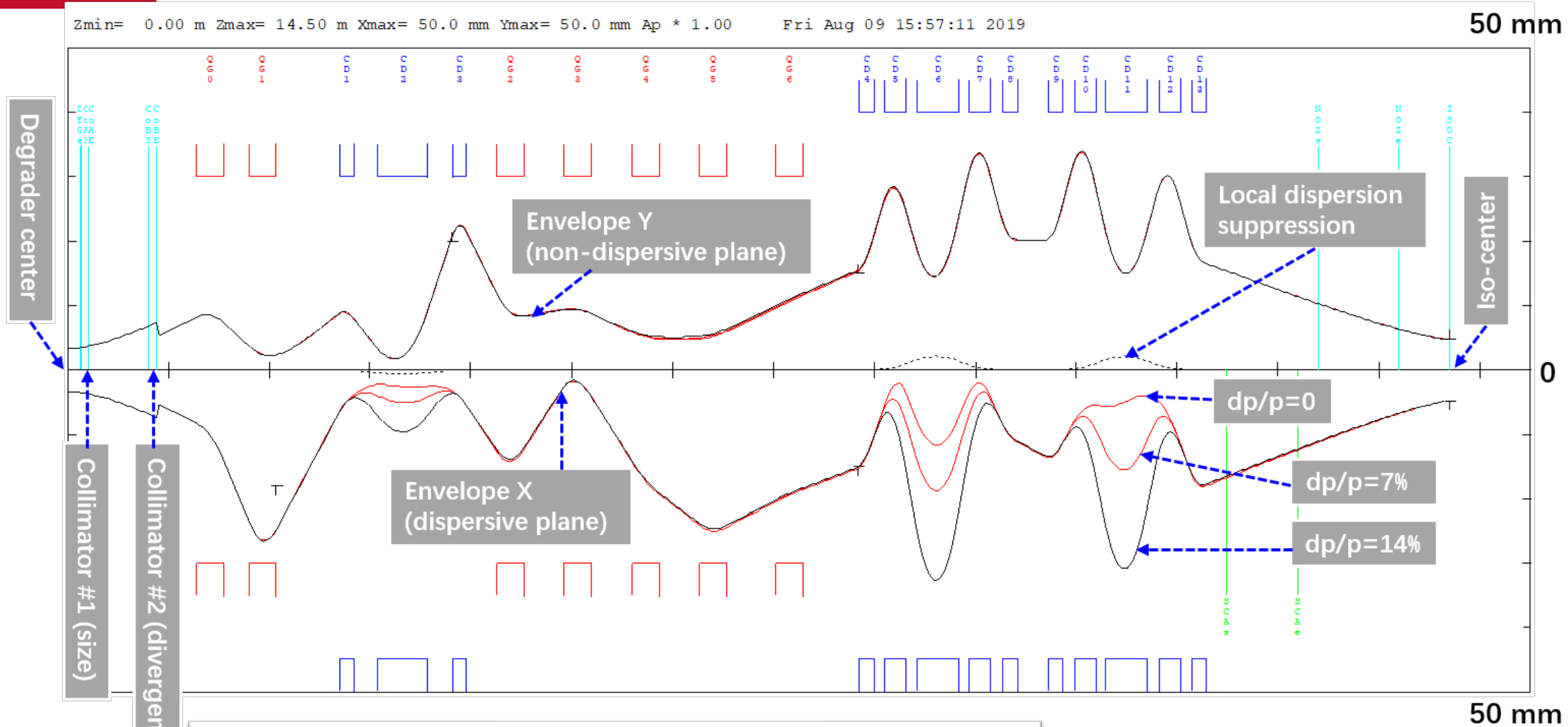
Features:

- SC Gantry can be configured as single-room PT or multi-room PT
- **Independent hybrid degrader** installed at the entrance of the gantry (without energy slit, max. 2.6% dp/p @ 70 MeV)
- **Downstream scanning**, avoid large aperture final dipole → reduced fringe field, minor contribution to aberrations.
- **SAD ~ 2.0 m**, with a compact nozzle

Magnets in gantry beamline

- ❑ AG-CCT combined function magnets are used for 2 bending sections: CB1 45 deg. ; CB2-A , CB2-B 67.5 deg. **Local dispersion suppression are used to achieve +/-14% momentum acceptance.**
- ❑ Q1-Q7 are resistive quadrupoles with small aperture.

SC Gantry optics



➤ Demonstration of a four-layer AG-CCT magnet

Table 1: Lattice parameters for CB1 45° AG-CCT magnet (F-D-F), and CB2-A/CB2-B 67.5° AG-CCT magnet (F-D-F-D-F)

| Type | No. | Bending angle | Field index n |
|--------------|--------|---------------|-----------------|
| 45° AG-CCT | #1 (D) | 8.2° | 25 |
| | #2 (F) | 28.6° | -25 |
| | #3 (D) | 8.2° | 25 |
| 67.5° AG-CCT | #1 (F) | 9.0° | 17.7 |
| | #2 (D) | 12.9° | -17.7 |
| | #3 (F) | 23.7° | 17.7 |
| | #4 (D) | 12.9° | -17.7 |
| | #5 (F) | 9.0° | 17.7 |

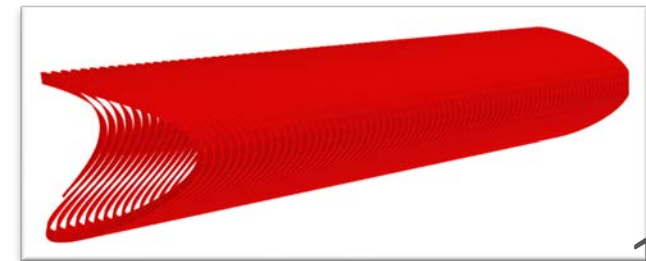
Dipole CCT Path

$$\vec{p}(\theta) = r\hat{r} + [rcot(\alpha)\sin(\theta) + \frac{\omega}{2\pi}\theta]\hat{z}$$



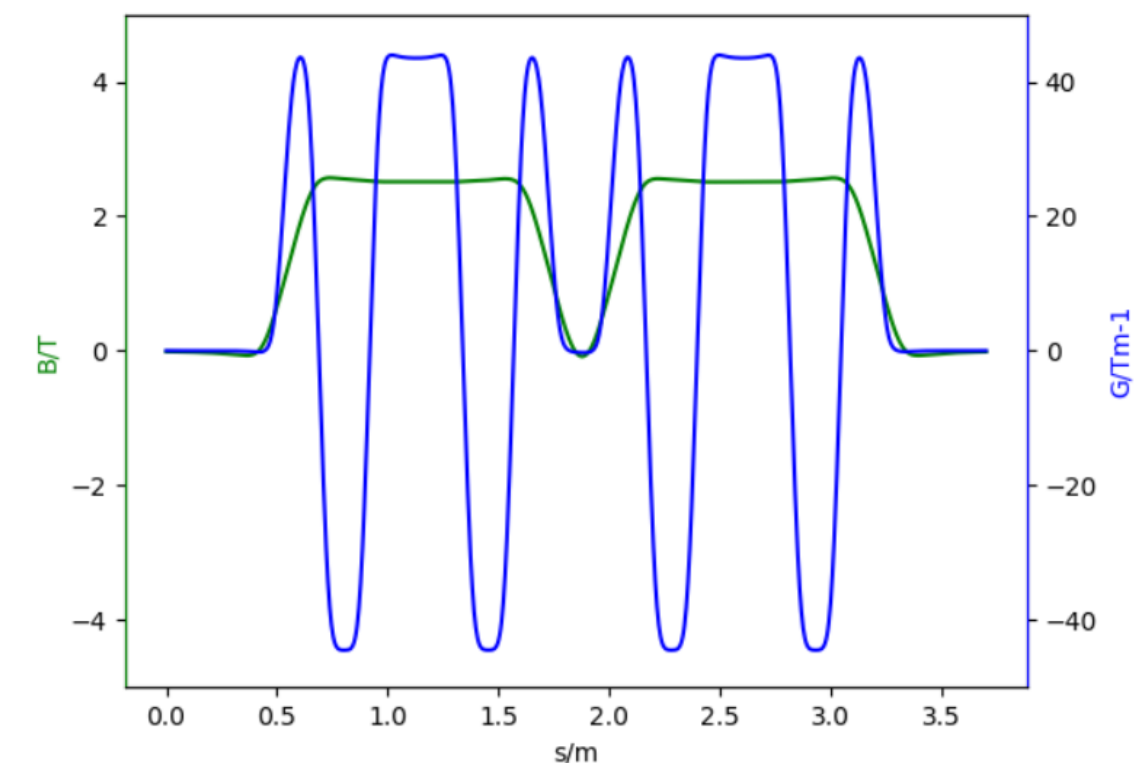
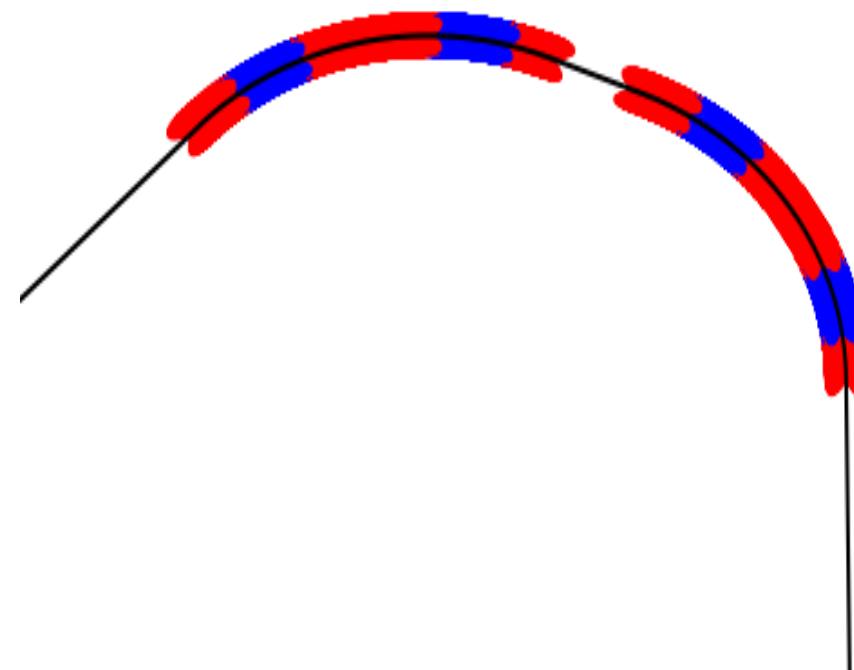
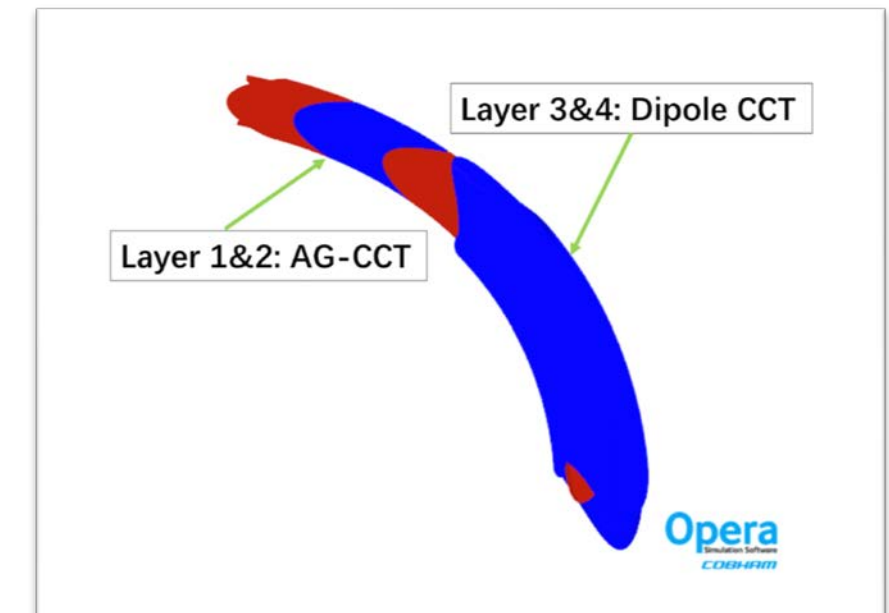
Quadrupole CCT Path

$$\vec{p}(\theta) = r\hat{r} + \left[\frac{rcot(\alpha)}{2}\sin(2\theta) + \frac{\omega}{2\pi}\theta\right]\hat{z}$$



Combined-function multipoles CCT modelling and field calculation

- ❑ OPERA-3D: time-consuming for complex multi-layers AG-CCT magnets, based on FEM (finite elements method)
- ❑ Due to pure coil induced magnetic fields without iron (ignoring stray field shielding and cross-talk effect), a **self-developed code based on Biot-Savart Law** was written for:
 - ✓ Parametric modelling of combined-function CCT magnets (dipole, quadrupole, sextuple CCTs).
 - ✓ Fast magnetic field calculation according to various precision requirement.
 - ✓ Runge-Kutta particle tracking, Visualization.



Dipole and quadrupole field distortion in curved CCTs

Curvature of curved CCT will break field symmetry along the radius in cross section, and lead to

(1) Small inherent quadrupole field, from dipole CCT

$$b_2^{inh} \approx b_1 / (2 \cdot \rho)$$

(2) For quadrupole field of AG-CCT → center deviation & focusing difference in outside and inside radius → nonlinear distortion on beam phase space

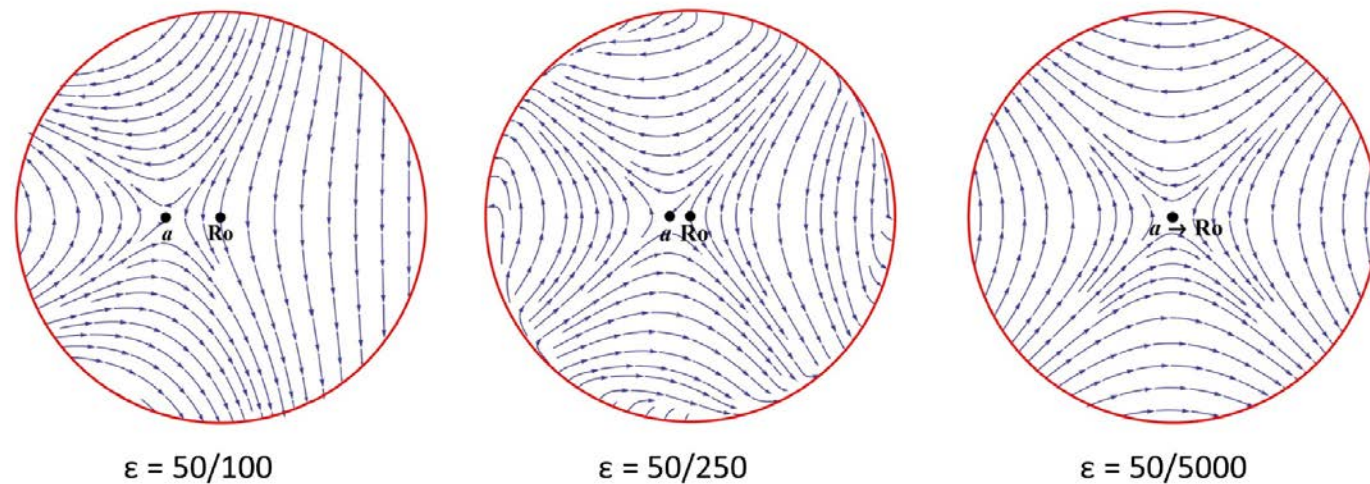
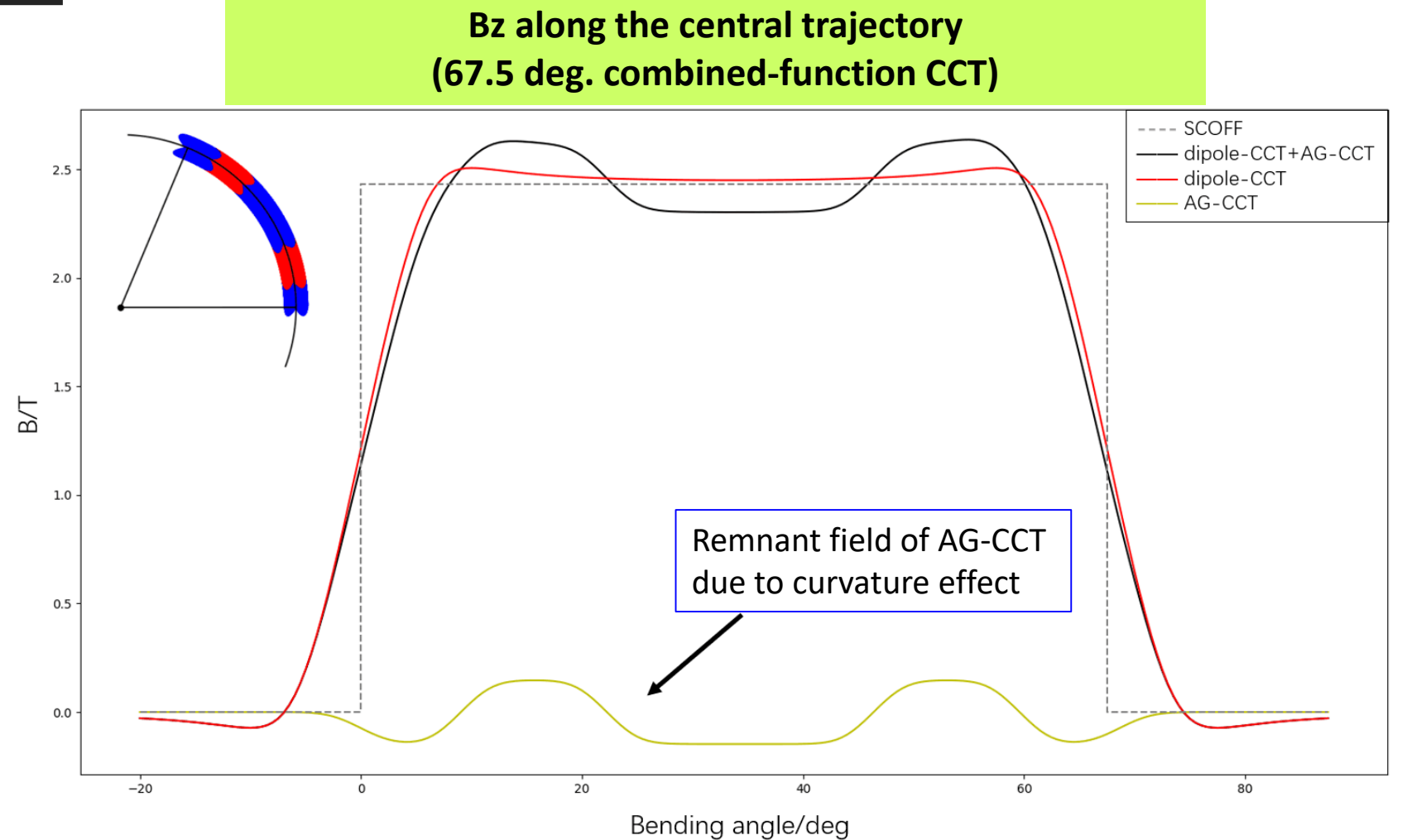
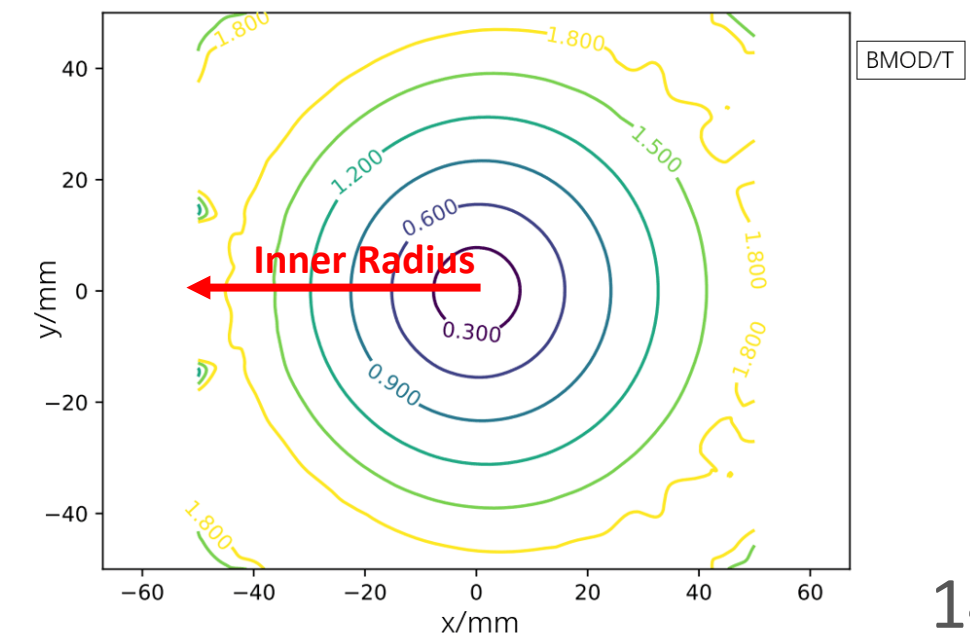


Figure 8.5: The quadrupole-like toroidal harmonic (n=2) is shown for a fixed bore radius R and increasing major radius R₀. The Legendre polynomials needed for the fields were evaluated using the DTOR algorithm [108]. As the aspect ratio of the torus ε = R/R₀ tends to zero, the fields are seen approaching those of a straight cylindrical quadrupole.

Lucas Nathan Brouwer, Canted-Cosine-Theta Superconducting Accelerator Magnets for High Energy Physics and Ion Beam Cancer Therapy, PhD Dissertation, UC Berkeley, 2015.



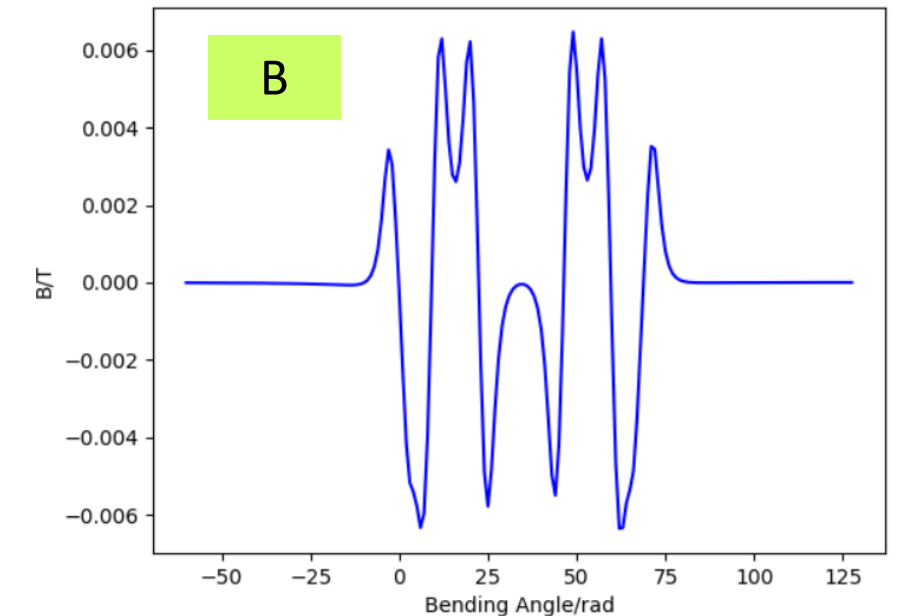
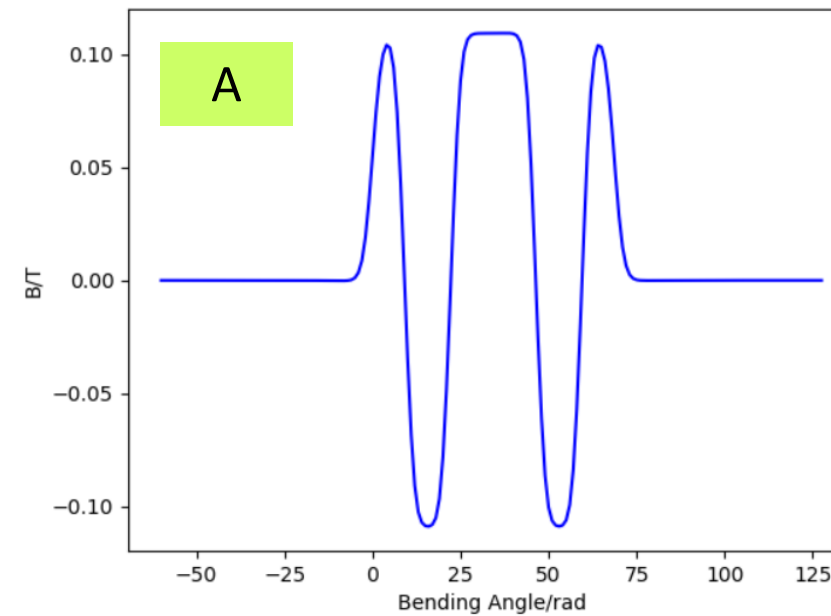
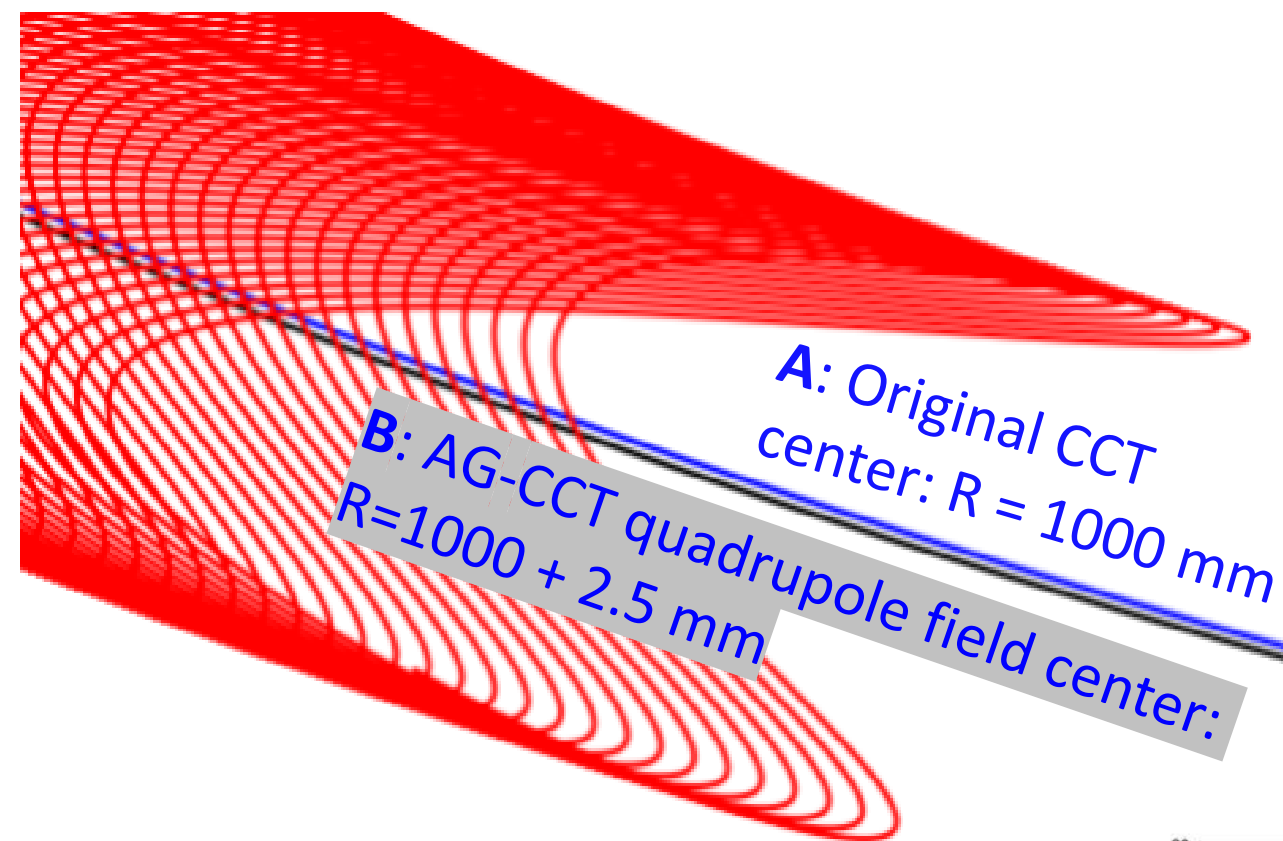
A compromise between the larger curvature (ρ) and higher dipole field is needed. For our case: ρ = 1 m, bore radius = 50 mm, b₁ = 2.43 T Off center = 2.5 mm



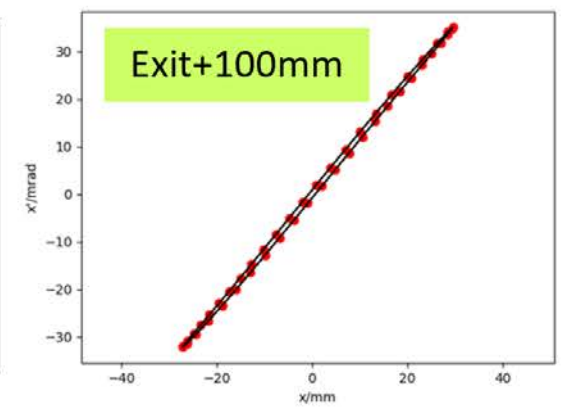
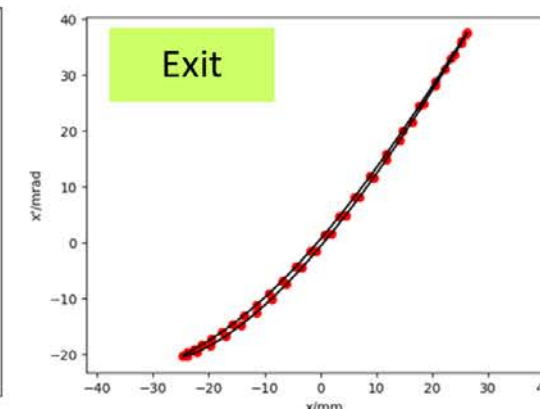
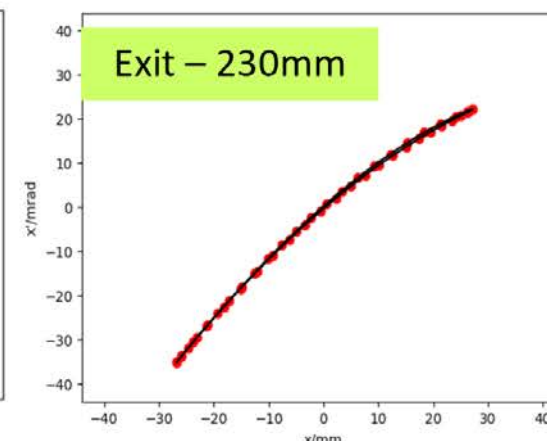
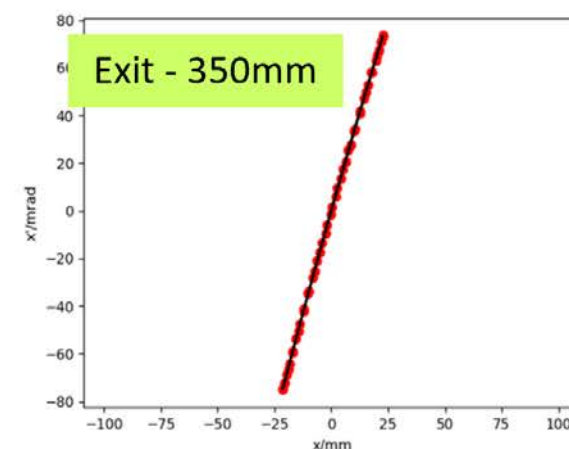
Isometric line of B_{mod} @ cross section of AG-CCT

Nonlinear effect on beam phase space

- One solution is to set a deviation for the central beam trajectory to the distorted quadrupole field center;
- However, due to the gradient distortion, the beam will have nonlinear focusing effect



Remnant dipole field distribution due to quadrupole field distortion in AG-CCT

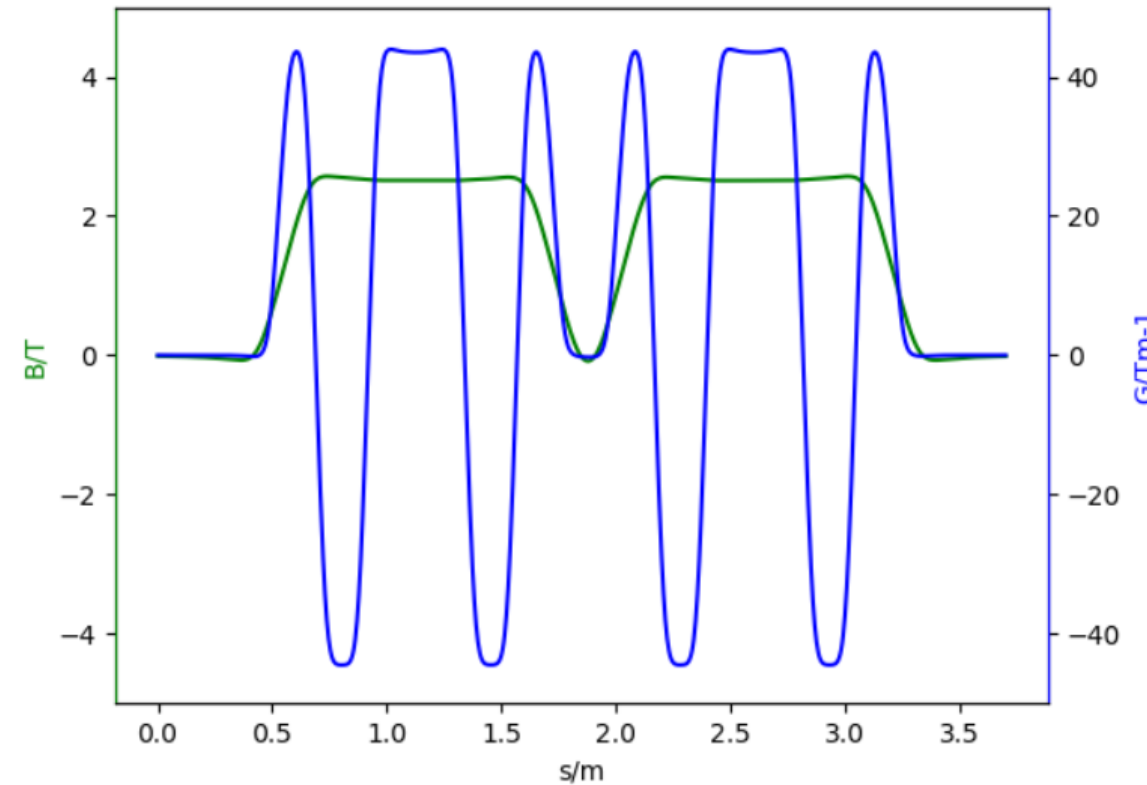
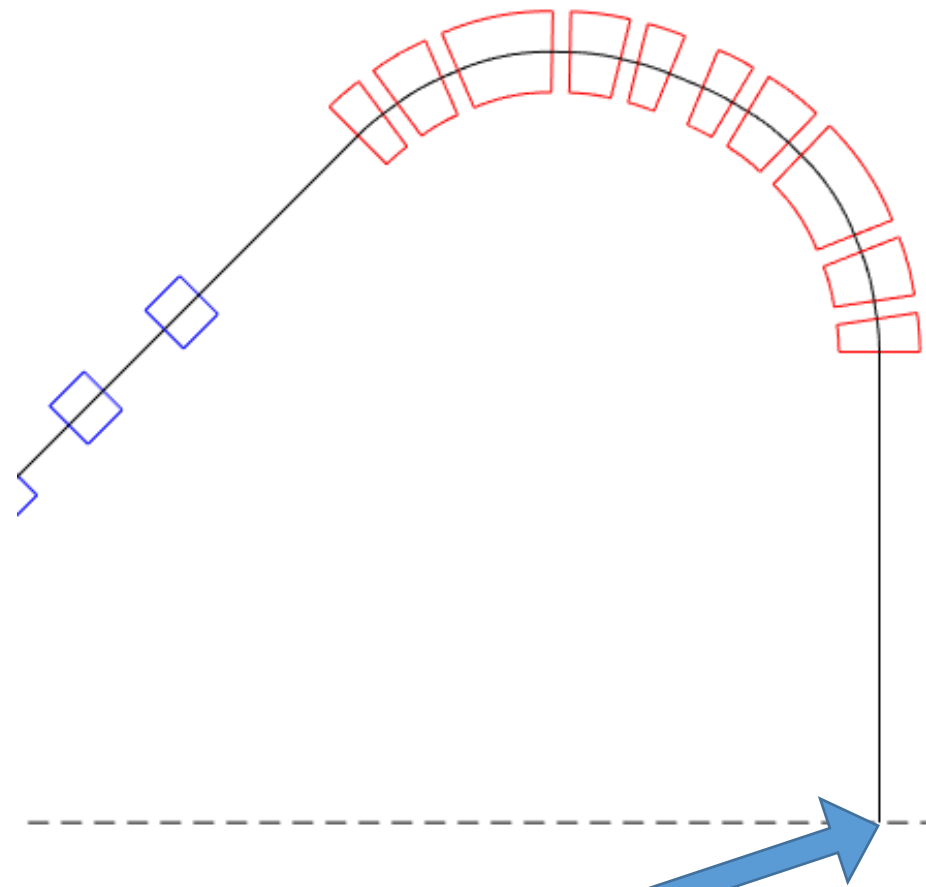


Phase ellipse evolution with nonlinear focusing effect, when passing one 67.5 deg. AG-CCT

Parameters of 67.5 deg. AG-CCT

For 67.5 deg. AG-CCT:

Max. dipole field: 2.43T; Max. gradient: 43T/m



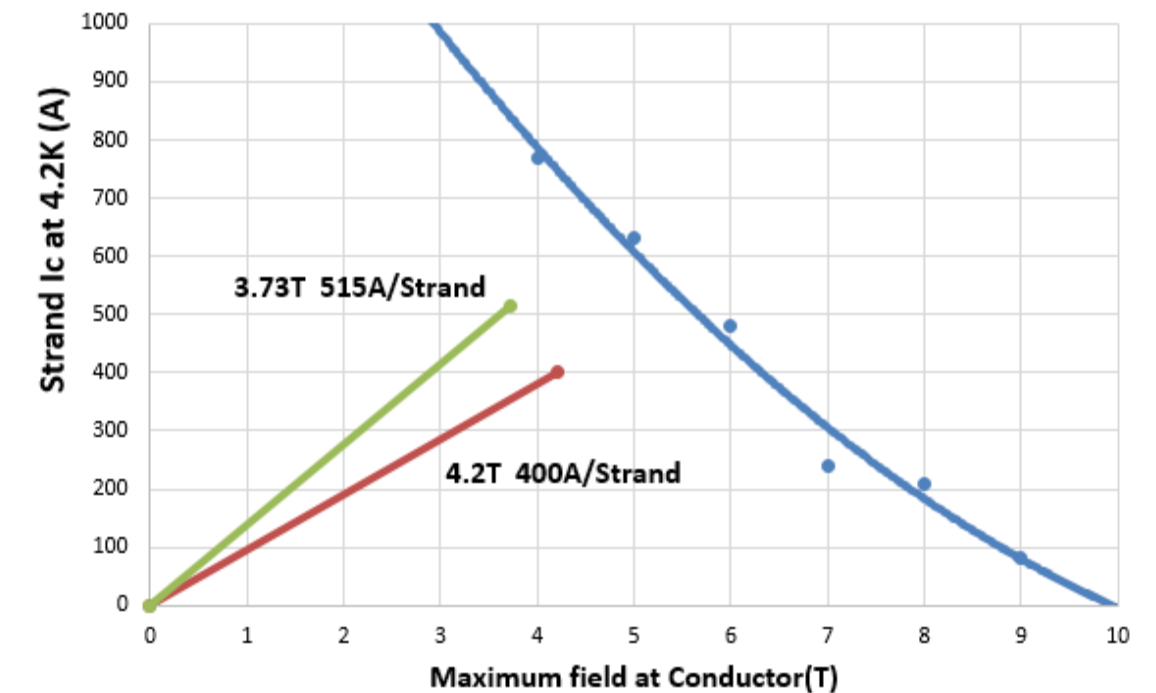
@Isocenter: Stray field 5.3Gs
(safety limit 5Gs)

Table 5 Parameters of the NbTi/Cu strand

| Superconducting wire | Parameter |
|-------------------------|-----------|
| Wire type | Monolith |
| Insulating material | Formvar |
| Bare dimensions/mm | 1.04 |
| Insulated dimensions/mm | 1.10 |
| Cu:Sc | 2.3 |
| RRR(273K/10K) | ≥100 |
| $I_c(5T, 4.2K)/A$ | ≥630 |

Table 6 Current margin at the maximum operating point

| Type | I/str.(A) | Str. | B_{cond} | Margin |
|-----------------|-----------|------|------------|--------|
| AG-CCT (L1) | 400 | 14 | 4.2T | 24% |
| AG-CCT (L2) | 400 | 14 | 4.2T | 24% |
| Dipole CCT (L3) | 515 | 12 | 3.73T | 21% |
| Dipole CCT (L4) | 515 | 12 | 3.36T | 26% |



Characteristic line of monolith NbTi strands

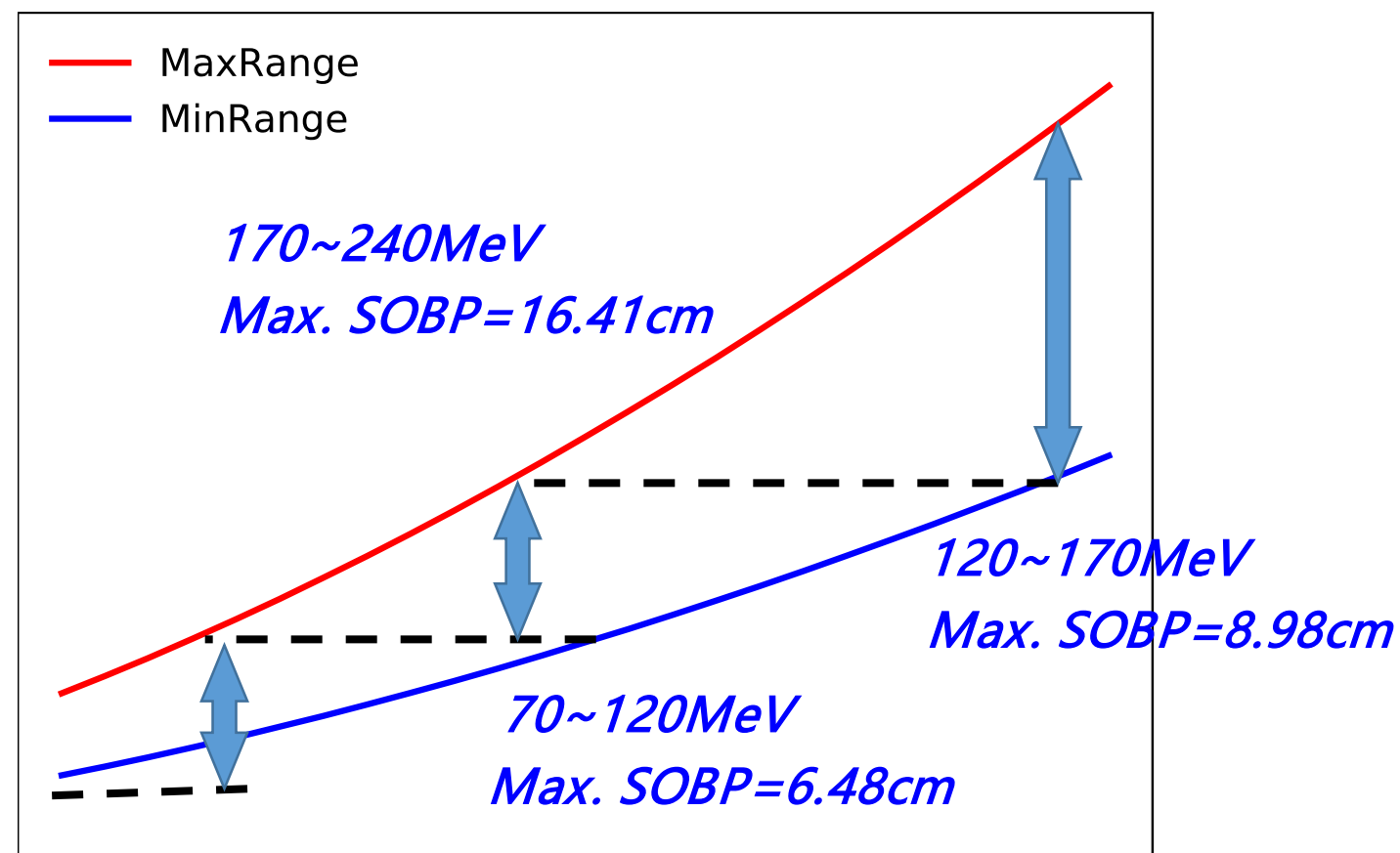
High order aberrations

- 2nd order aberrations has been studied using COSY Infinity. Present results show that aberrations have significant influence on beam optics, especially for large momentum offset situation.
- The original linear optics need be re-optimized in high order situation, and sextupole components will be introduced to minimize the aberrations.

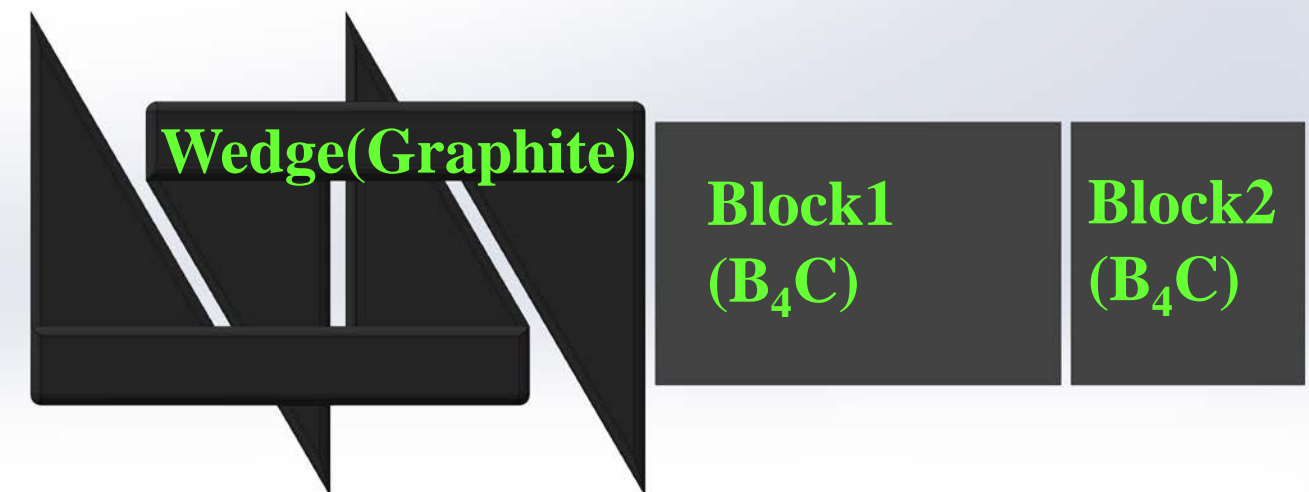
Hybrid structure degrader

□ $dp/p = \pm 14\%$ with linear optics; final $dp/p = \pm 10\%$ is assumed \rightarrow 4 central energy for CCTs

| Set Energy/MeV | dP/P | dE/E | E _{min} /MeV | E _{max} /MeV |
|----------------|--------|--------|-----------------------|-----------------------|
| 75 | 10.00% | 19.26% | 60.56 | 89.44 |
| 105 | 10.00% | 18.99% | 85.06 | 124.94 |
| 145 | 10.00% | 18.66% | 117.94 | 172.06 |
| 205 | 10.00% | 18.21% | 167.68 | 242.32 |



Energy Degradator in 3 stages:



□ 170~240MeV: Wedge

□ 120~170MeV: Wedge + Block1

□ 70~120MeV: Wedge + Block1 + Block2

Beneficial:

□ Higher transmission, for low-z materials usage of B₁, B₂ (B₄C, Be)

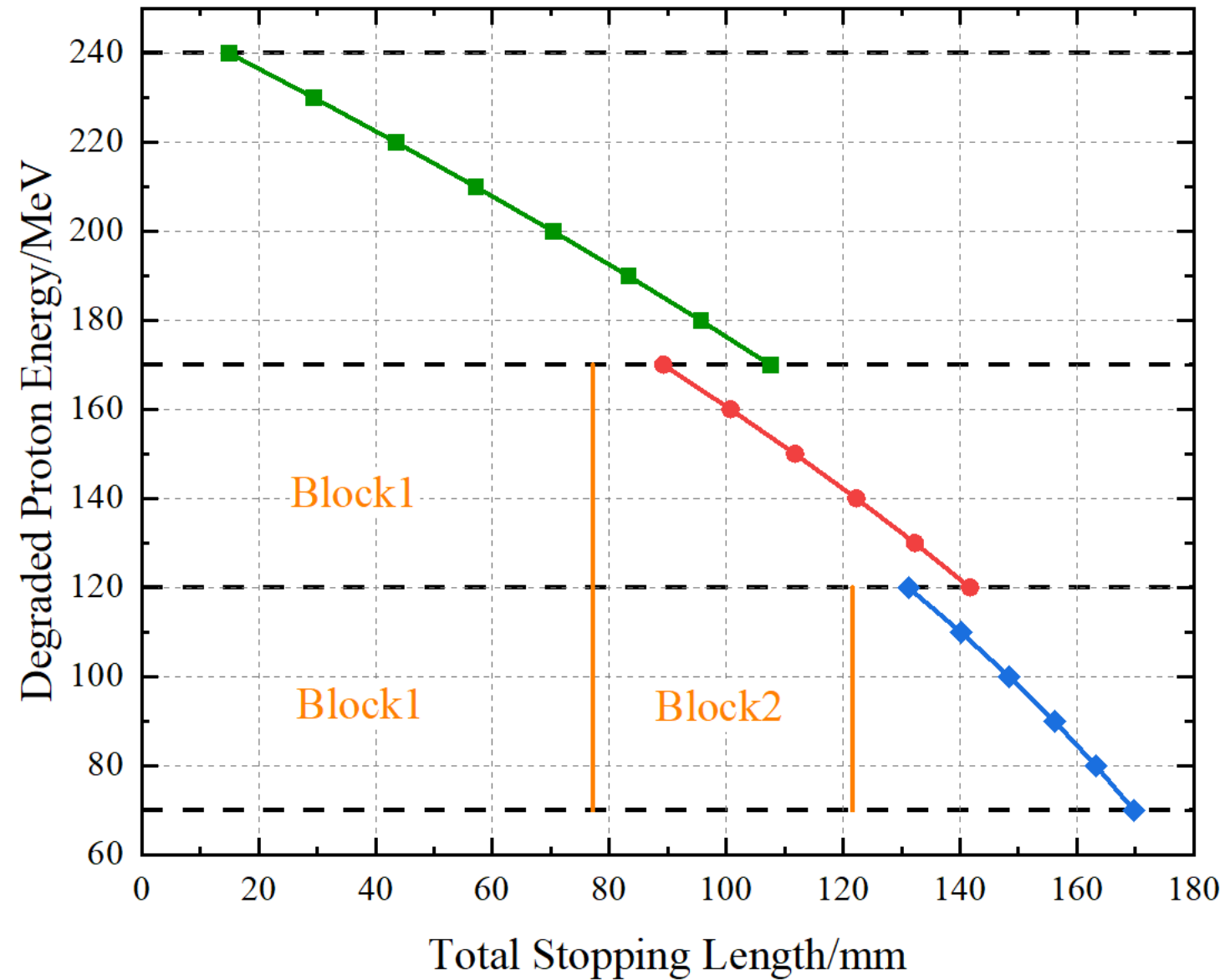
□ Lighter wedge (~1/4 of full wedge), higher motion speed

Hybrid structure degrader

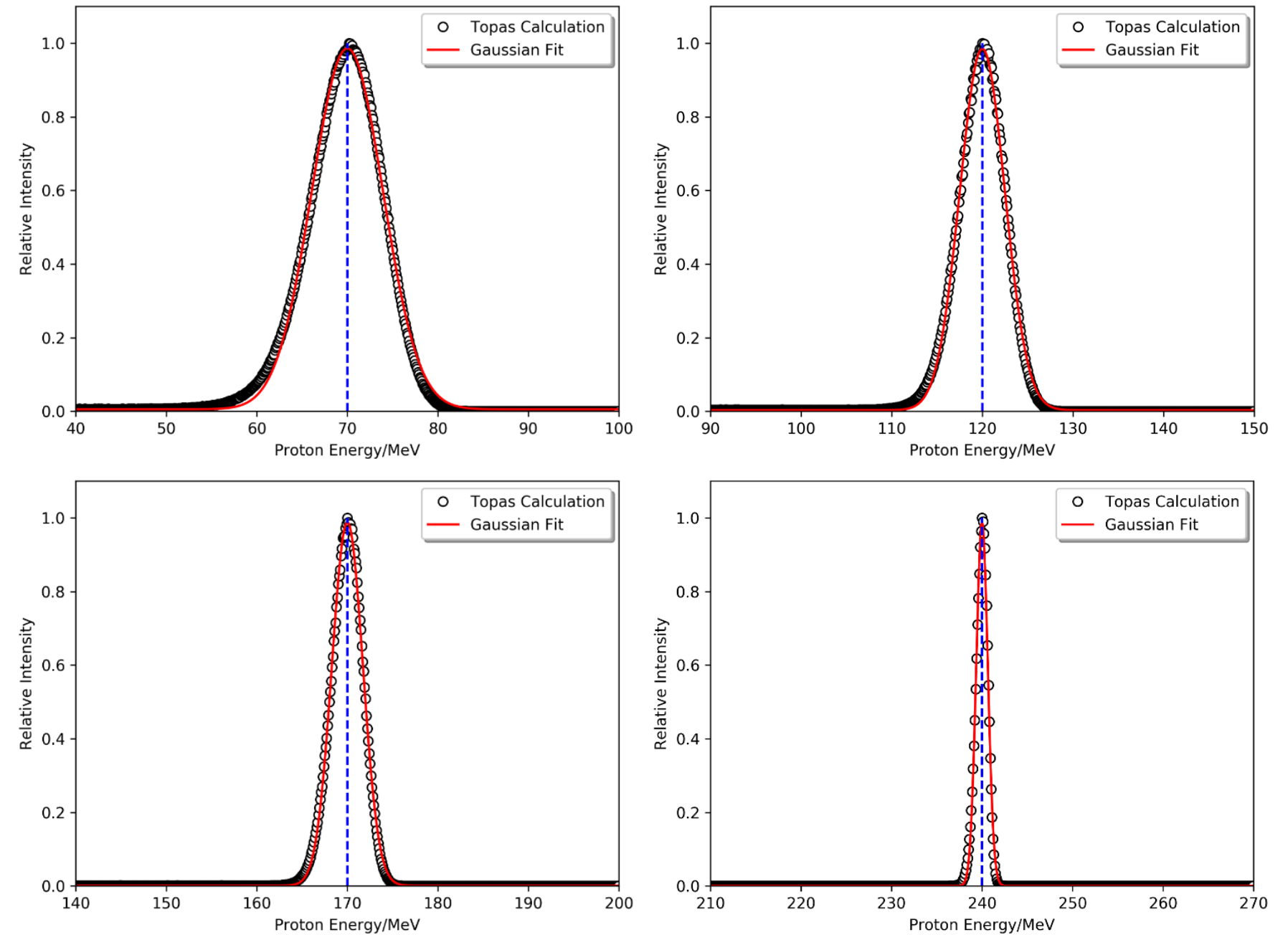
For continuous energy degrading:

□ Block1(B4C): 250MeV→180MeV

□ Block1+Block2: 250MeV→130MeV



Energy Spread After Degradator: 70, 120, 170, 240 MeV

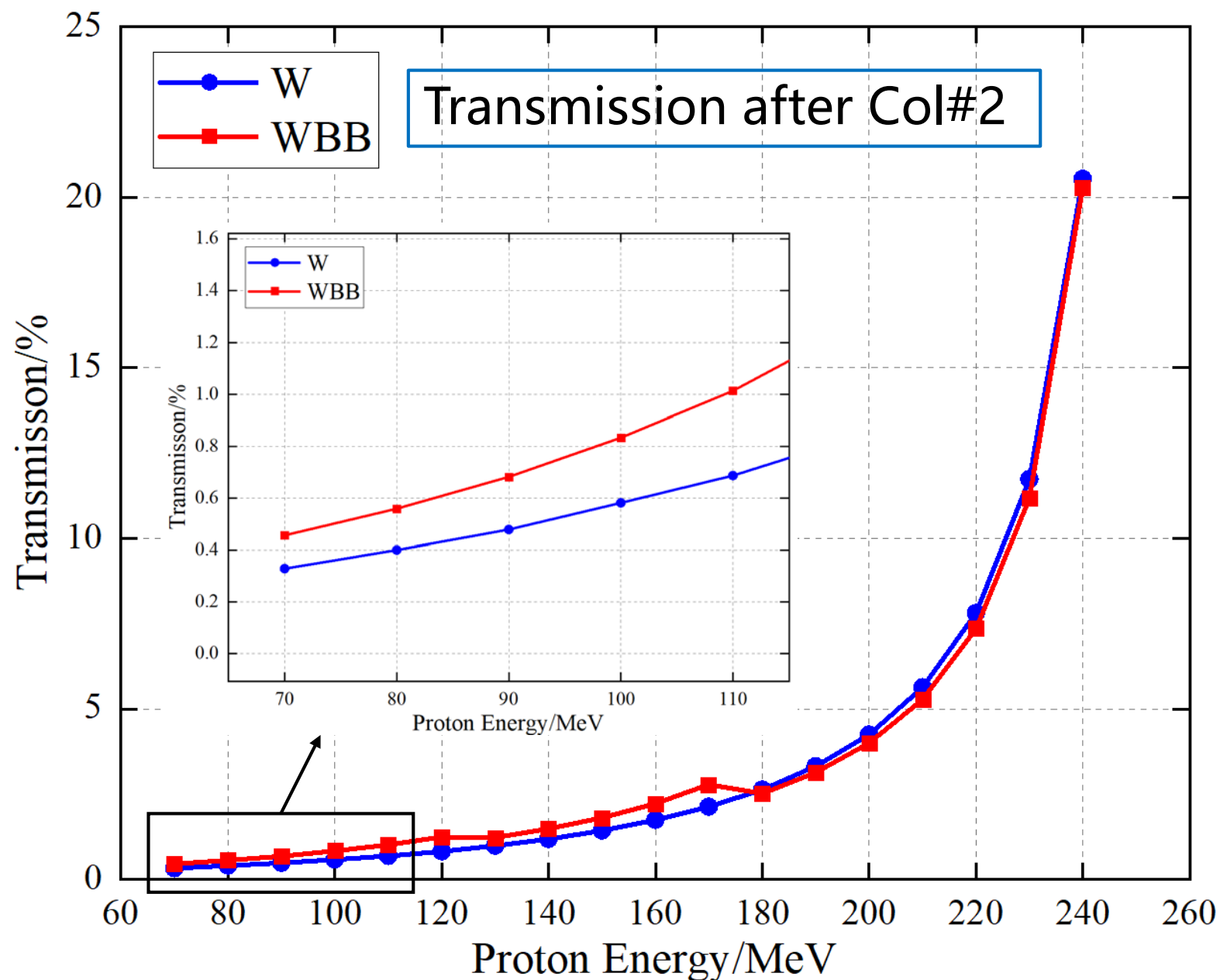


Transmission optimization of the hybrid degrader



After Collimator #2:

- Beam energy: 70-240MeV
- r.m.s. beam emittance: 7π mm*mrad



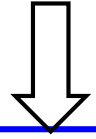
Compared to multi-wedge case:

□ 39~50% increase(relatively) for 70-120MeV

□ 24~30% increase(relatively) for 130-170MeV

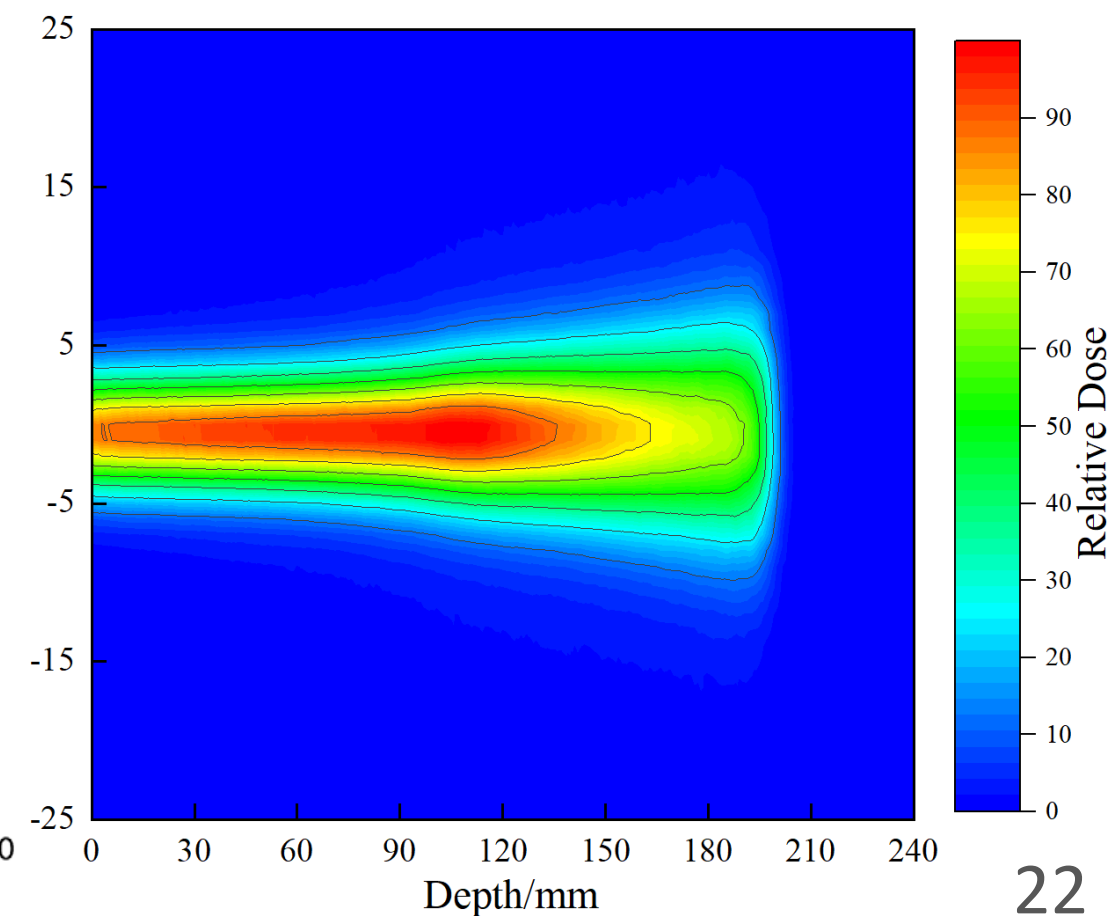
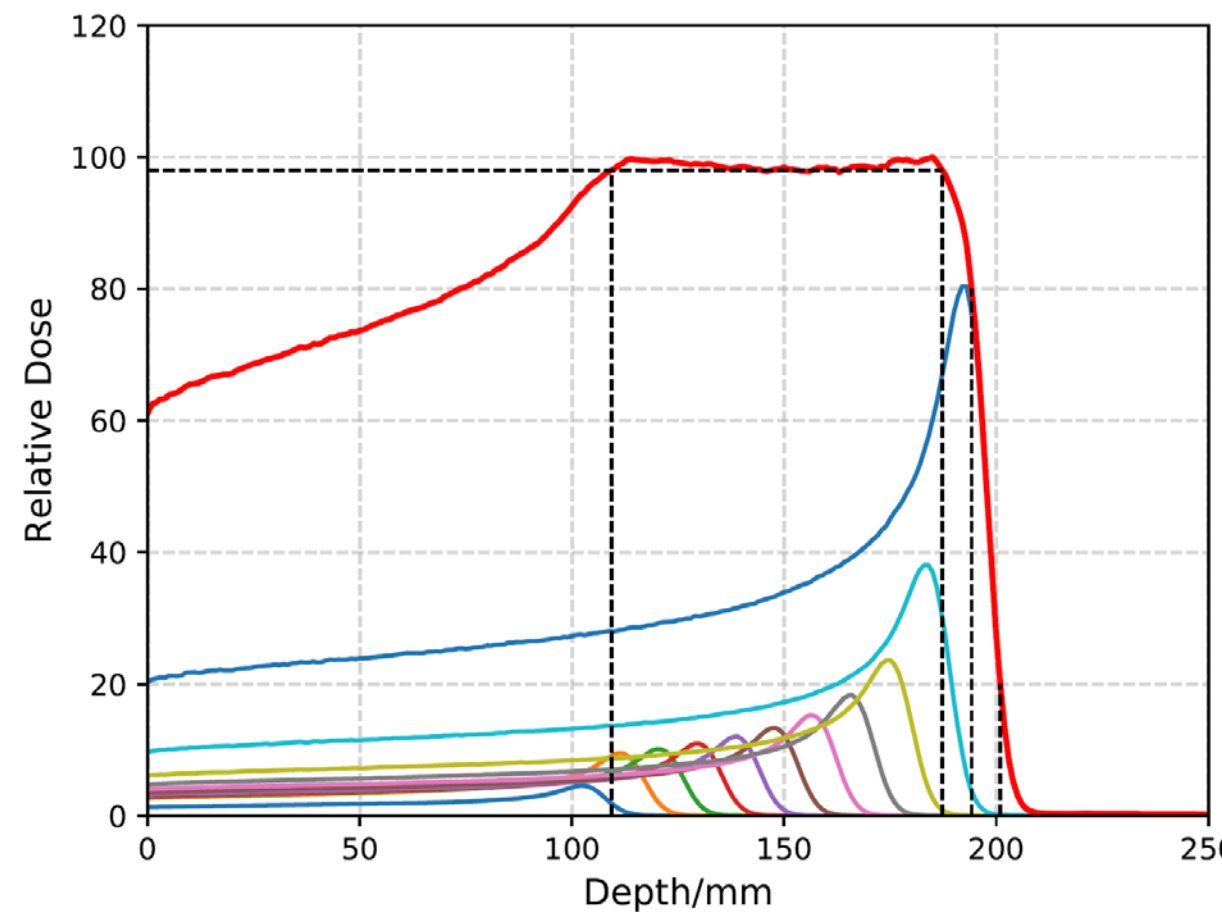
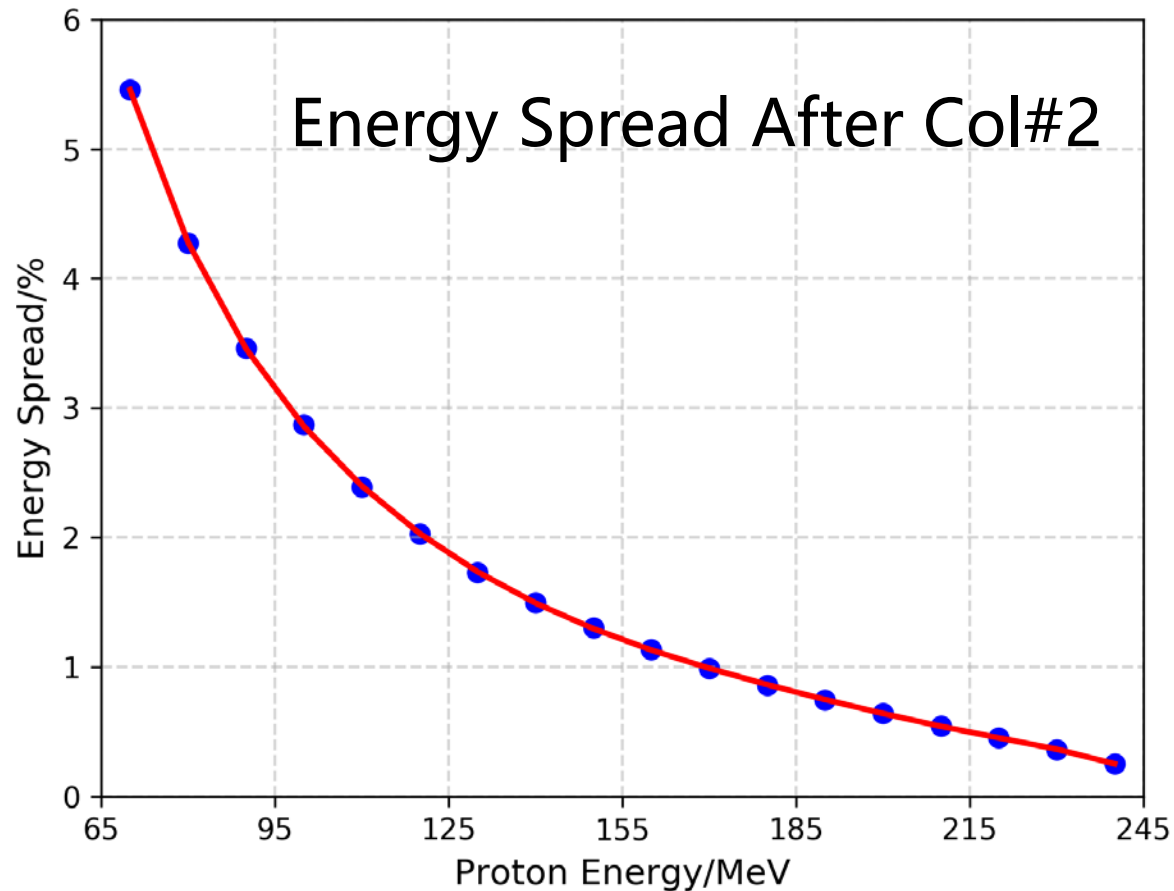
Beneficial from natural large energy spread

Larger energy spread \Rightarrow Larger distal fall-off \Rightarrow Range straggling: $\frac{dR}{R} = 3.3 \frac{dE}{E}$



- ✓ Larger distance between successive energy layers is possible
- ✓ Reduce overall energy change time

- SOBP Simulation (using TOPAS)
- Proton Energy: 120MeV -170 MeV ~ Range(10.5cm - 19.5cm)
 - Depth of Energy Layers: 10mm \rightarrow Energy Step: 11
 - W98=78mm W(d80 \rightarrow d20)=6.62mm



Conclusion

- For future research and development, we proposed a combined function AG-CCT gantry beamline, with large momentum acceptance and smaller footprint.
- Linear optics and influence of field imperfection from small-curvature AG-CCTs were studied. Considering field complexity and large momentum offset, high order aberrations with fringe field effect need be investigated and optimized.
- Combination of large momentum acceptance and natural energy spread during degrading (without energy slit), may lead to potential applications on fast 3D scanning.



Thank you for your attention!

Bin Qin, bin.qin@hust.edu.cn

Posters, this conference

Xu Liu et al., Design of a fast energy degrader for a compact superconducting gantry with large momentum acceptance

Runxiao Zhao et al., Design and optimization of beam optics for a superconducting gantry